BOLUS LIBRARY
C31 0000 0645

65-706.

Biophysical Interactions in the Iceland Basin

Amy Harington

Supervisor: Mike Lucas

A dissertation submitted to the University of Cape Town, in partial fulfilment of the requirements for the award of an Honours degree in Ecology

October 2008

KD HARI

The copyright of this thesis vests in the author. No quotation from it or information derived from it is to be published without full acknowledgement of the source. The thesis is to be used for private study or non-commercial research purposes only.

Published by the University of Cape Town (UCT) in terms of the non-exclusive license granted to UCT by the author.

University of Cape Town

Biophysical Interactions in the Iceland Basin

Abstract

The Iceland Basin in the N. Atlantic has attracted considerable recent attention because the spring bloom in this region acts as the most powerful biological carbon pump anywhere in the world oceans.

Furthermore, the link between primary productivity and herbivory by the calanoid copepod, *Calanus finmarchicus* provides the trophic link between primary producers and the important commercial fishery for Atlantic Cod. However, one result of ocean warming is that the distribution of the cold water loving *Calanus finmarchicus* is being pushed northwards which adversely affects the food supply to juvenile Cod. Perhaps of more serious concern are concerns that the biological carbon pump may weaken as a result of increased thermal stratification and therefore reduced upward nitrate flux to drive nitrate-based export production.

This was in fact confirmed at least in the study region which is dominated by regenerated production (f-ratio <0.5) which in turn suggests a shift in community structure from larger celled organisms to smaller celled organisms, characterised by long inefficient food chains.

This project makes use of summer cruise data to the Iceland Basin last summer (2007) where measurements of 15N derived new production (NP) were made to add to previous seasonal (spring, winter) measurements of NP in the region.

Introduction

Phytoplankton play an important role in the global carbon cycle and in climate regulation by converting CO_2 to organic carbon in the surface oceans that may then be exported into the deep ocean by vertical particle flux, where carbon is then stored for long periods of time without the opportunity to ventilate CO_2 back into the atmosphere (Chisholm et al. 2001, Falkowski et al. 1998). Although phytoplankton account for less than 1% of photosynthetic biomass globally, they are responsible for roughly half of the carbon fixation on Earth (Falkowski et al. 2000). Most of the organic carbon phytoplankton produce is eaten by other organisms in surface waters, and thus much of the ingested carbon is respired, leading to CO_2 evolution and a potential source back into the atmosphere as these organisms respire. However, some organic carbon (POC) sinks to the deep ocean, thus reducing CO_2 in the surface layer and elevating it in the deep sea (Chisholm et al. 2001). A CO_2 concentration gradient is therefore maintained by the "biological pump" as it removes CO_2 from the atmosphere and stores it in the deep ocean (Chisholm et al. 2001). The Iceland Basin in the North Atlantic exhibits the strongest 'biological carbon pump' in any of the world oceans (Lucas et al. 2008)

Various factors influence the efficiency of the 'biological pump' and one of the most prominent factors affecting its operation is phytoplankton community structure. The biological pump acts most efficiently where a community is dominated by larger celled phytoplankton such as diatoms (Probyn 1987) which also determines an ecosystem's ability to function, particularly with respect to efficient energy transfer through food chains (Anderson & Lucas 2008). Whether a community is dominated by diatoms relative to smaller cells such as phytoflagellates is indicative of environmental factors such as nutrient availability which is controlled by the degree of ocean stratification or by the stage of upwelling cycles. Phytoplankton community structure shifts from one dominated by diatoms to one dominated by smaller cells as nutrients become depleted (Anderson & Lucas 2008), and this shift will determine the efficiency of the 'biological pump' as well as the ecosystem's ability to support commercially important fisheries (Anderson & Lucas 2008).

Export production in high latitudes is often dominated by diatoms (Dugdale et al. 1995) because of their ability to rapidly take up (and temporarily store) nutrients for growth (Falkowski 1998), thus leading to characteristic spring blooms. However, once diatom blooms become nutrient and / or light limited, the fact that they are heavily silicified means that they sink rapidly (Francois et al. 2002) when they die; thereby rapidly exporting POC (& PON) into the deep ocean, ensuring that the biological carbon pump operates efficiently.

The two most important factors that control phytoplankton growth are light and nutrient (specifically NO_3 PO_4 and Si) availability (Mitchell-Innes et al. 2001). Smetacek (1998) showed that diatom productivity is most limited by inorganic nitrogen availability, and because of its speciation into oxidised and reduced forms, this has led to the emergence of one of the most well-know paradigms in modern biological oceanography; the concept of "regenerated" and "new" production (Dugdale & Goering 1967). New production is primary production based on the uptake of nitrogen which is "new" to the euphotic zone (Probyn 1992), i.e. primarily nitrate advected into surface waters from below and / or di-nitrogen (N_2) fixed by nitrogen fixers from the atmosphere. Conversely, "regenerated" production is primary production based on the uptake of reduced or re-cycled nitrogen (from excretion) such as ammonium, urea or dissolved free amino-acids (DFAA). The significance of considering the relative proportions of new versus regenerated production is that new production based on nitrate uptake (ρNO_3^-) has (historically at least) been equated with PON export over appropriate time and space scales since the upward flux of NO_3^- must balance the downward flux of PON if the ocean mass balance of N is to be maintained – but making the important assumption that PON mineralisation to NH_4^+ and its subsequent nitrification to NO_3^- occurs only in the aphotic layer. Thus measurements of ρNO_3^- by phytoplankton can be used to infer carbon export if some assumptions about cellular Redfield stoichiometry (C:N; 6:1) are invoked. Frequently, and certainly in the past, the magnitude of the potential for carbon export has been described by the f-ratio, that is new production as a fraction of total production, i.e.: ρNO_3^- / ρNO_3^- + ρNH_4^+ + ρurea; where an f-ratio value of >0.5 signifies predominantly new (i.e.

export) production, while an f-ratio value of <0.5 signifies primarily regenerated production. However, recent evidence for euphotic layer nitrification rates has somewhat undermined the value of using the f-ratio to estimate export rates, although it remains a useful concept to describe phytoplankton community structure and the likely routes for energy transfer to higher trophic levels (Yool et al. 2007).

Global interest in iron-limited phytoplankton growth rates and the impact that this has on the biological carbon pump can however also be explored through the f-ratio. Rates of ρNO_3^- uptake, and more importantly specific nitrate uptake (V_{NO3} d^{-1}; i.e. turnover times), provide evidence for potential Fe-limitation of phytoplankton growth since nitrate assimilation requires the enzyme nitrate and nitrite reductase that is Fe-dependent (Lucas et al., 2007). In this context it is clear that the efficiency of the biological pump is therefore dependent both on rates of new production and how this might be limited by Fe-availability.
Many aspects of phytoplankton N metabolism are well known iron dependent process (Raven, 1980, 1990; Sunda & Huntsman, 1997; Boyd et al. 1999; De Baar et al. 2005 cited in Lucas et al. 2007). Iron limitation can lead to stunted growth and incomplete drawdown of macronutrients into the deep ocean (Moore et al. 2006). Evidence states that nitrate uptake is Fe-limited in many of the world's oceans (Southern Ocean, Equatorial Pacific, Pacific Subpolar gyre and some coastal upwelling regions) (Martin & Fitzwater, 1988; Coale et al., 1996; Hutchins & Bruland, 1998; Boyd et al., 2000, 2004; Tsuda et al., 2003 cited in Moore et al., 2006). The North Atlantic typically has a low iron to nitrate ratio in upwelled (winter-mixed) waters and so the spring bloom results in the incomplete removal of nitrate from the mixed layer in some regions. Although supplementation of upwelled Fe concentrations by mineral aerosols had previously been considered sufficient to remove the possibility of Fe-limitation playing a role in phytoplankton growth and production in the North Atlantic, recent evidence presented by Moore et al. (2006) suggests that certain regions of the North Atlantic are in fact iron limited. This suggests that aeolian iron supply has a much more significant role than previously thought

in controlling the spring bloom progression as well as size-based community structure.

As ambient iron concentrations become limiting in surface waters, new production should become dominated by smaller cells which have a greater surface area to volume ratio to ensure optimal nutrient uptake (Smetacek, 1998). However, such a shift in community structure would seem likely to render the biological carbon pump less efficient since smaller cells will sink more slowly and be subject also to greater mortality due to microzooplankton grazing (Price et al., 1994; Smetacek et al., 2004, Lucas et al., 2007). Further, a high f-ratio is most likely associated with large cells and 'new' iron inputs, whereas a low f-ratio would be associated with smaller cells and 'regenerated iron inputs' (Lucas et al., 2007). Thus the variability in the timing and magnitude of the spring bloom in the Northern Atlantic may be strongly influenced by the supply of aeolian iron supply with impacts on carbon drawdown (from nitrate new production) and food web dynamics (Lucas et al., 2007).

Phytoplankton form an important part of the food web for marine mammals and for commercially important fish such as cod (Richardson and Schoeman, 2004). In the northeast Atlantic, global warming has resulted in sea surface warming which has in turn resulted in increasing phytoplankton abundance in cooler regions and decreasing phytoplankton abundance in warmer regions (Richardson & Schoeman, 2004). This shift results in bottom up impacts through the ecosystem, from copepod herbivores to zooplankton carnivores because of tight trophic coupling (Richardson & Schoeman, 2004), with likely strong negative consequences on already-depleted fish populations.

Additionally, the affect of changing weather on the intensity of ocean mixing (and conversely stratification) will influence light levels, surface temperatures and the amount of nutrient recycling from deep layers which in turn has knock-on effects on phytoplankton growth that in turn drives bottom-up processes throughout the pelagic food chain (Richardson & Schoeman, 2004; Hayes et al., 2005). In the northeast Atlantic, *Calanoid* copepod assemblages

have displayed very obvious biogeographical shifts in the past 40 years, with warm-water assemblages moving as much as 1000km northwards while there has been a simultaneous retraction in the range of cold-water assemblages (Hayes et al., 2005). Recent poor recruitment of cod is thought to be partially linked to the recurrence of small copepods (Hayes et al., 2005).

Currently, many scientists are seriously concerned that as a result of global warming and therefore increased thermal stratification that may lead to reduced upward nitrate flux to drive nitrate based export production, the biological carbon pump may weaken. This negative impact may be exacerbated if nitrate uptake is Fe-limited. The aim of this investigation is therefore primarily to assess the potential for carbon export in the Iceland Basin of the North Atlantic by measuring new production rates using ^{15}N stable isotope labelling techniques. Secondarily, the aim is to evaluate whether or not new production in this region is iron limited, because future trends in aeolian dust transport into the oceans will tend to predict whether rates of new production are likely to increase or to diminish in the future. Finally, the dominant copepod in the Icelandic Basin, *Calanus finmarchicus,* is a herbivore feeding primarily on diatoms and is the major food resource for juvenile cod, the most important commercial fin-fish of the region. Clearly any adverse effects on new production rates will have direct and negative effects on cod recruitment.

Materials and Methods

Study site and productivity stations

Nitrogen uptake and carbon fixation measurements of phytoplankton productivity were made within the Iceland Basin in the North Atlantic on 13 separate days from 30 July to 21 August 2007. The aim was to assess production rates as a function of available light and macronutrient (N, Si, P) concentration as well as to determine whether production was iron limited. Two types of productivity measurements were performed in on-deck simulated *in situ* incubators using stable isotopes; these being 'new' and 'regenerated' (^{15}N labelled) light and dark nitrate and ammonium uptake

experiments respectively as well as ^{13}C primary production measurements. The experiments were performed at 6 different light depths (55, 33, 14, 7, 4.5 and 1%) representing *in situ* underwater irradiance. Ammonium regeneration rates were also measured at each station to correct the ammonium uptake rates for isotopic dilution.

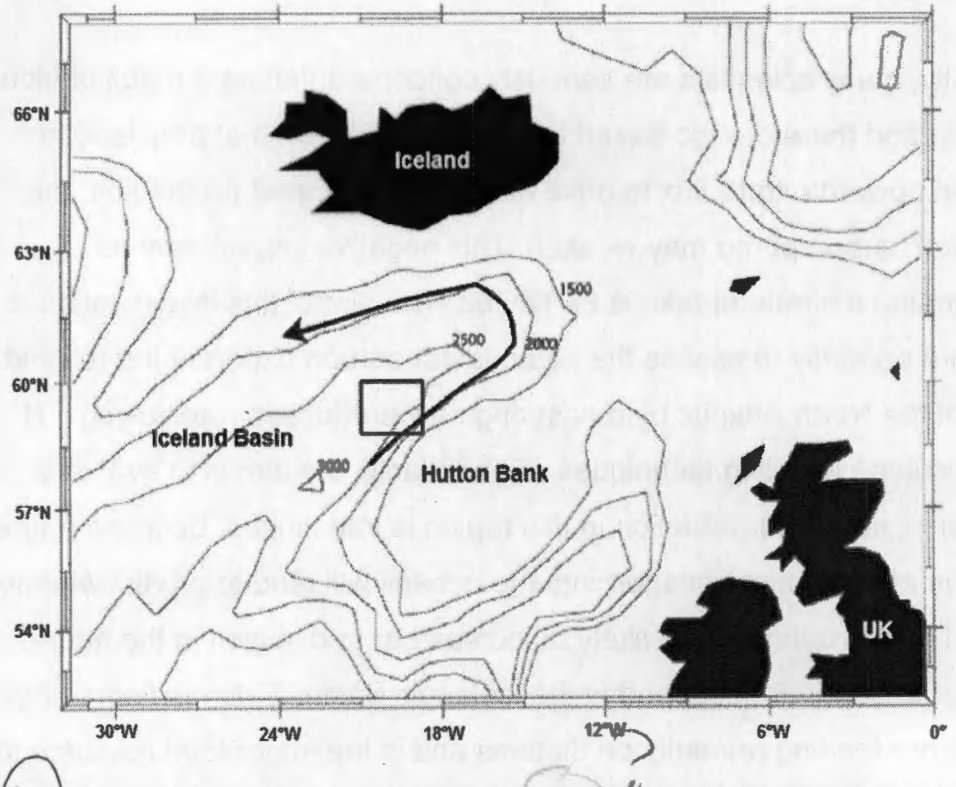

Figure 1: Map of study area (indicated by red square) with depth contours at 500m intervals from 3000m to 1500m for reference.

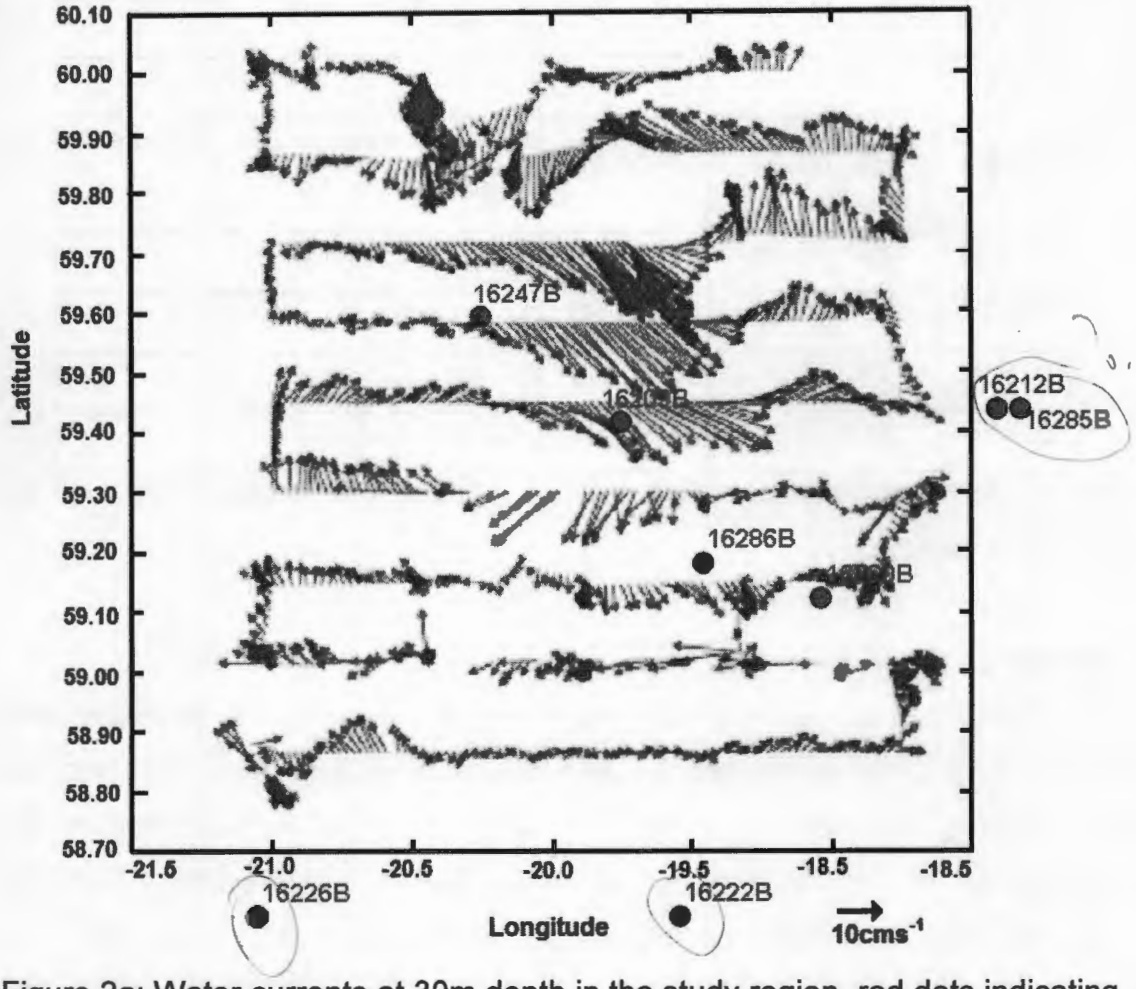

Figure 2a: Water currents at 30m depth in the study region, red dots indicating stations sampled. Eddy dipole consisting of a cyclonic eddy at 59.80°N, 19.75°W and an anticyclonic eddy at 59.40°N, 20.25°W with a region of high current sheer in-between them.

Discovery station no.	Latitude	Longitude	Date
16209B	59° 42.12	20° 25.65	30 July
16212B	59° 42.66	18° 45.09	31 July

16222B	58° 51.80	19° 52.95	2 August
16226B	58° 51.40	21° 00.64	4 August
16235B	59° 08.90	19° 52.96	9 Aug., Filament + turbulence profiles
16247B	59° 59.93	20° 27.20	10 Aug., Filament
16260B	59° 11.71	19° 05.96	12 August
16285B	59° 40.26	18° 43.56	18 Aug., N Eddy
16286B	59° 16.40	19° 47.60	19 Aug., S. Eddy

Figure 2b: Positions of sampling stations (latitude and longitude) as well as the dates sampled

Sampling

To ensure that iron contamination was minimised during the collection and manipulation of the water samples, all samples were drawn from acid-cleaned NIO bottles attached to a titanium CTD (Ti-CTD) frame following its deployment at the "productivity" stations. New 2-1 acid-washed Nalgene polycarbonate incubation bottles sealed within Ziploc bags were used to decant the CTD bottle sample water drawn from each of the 6 light depths (55, 33, 14, 7, 4.5 and 1%) directly. A dedicated trace metal clean container lab containing a Class-100 laminar flow hood was used to perform the spike additions, after which the incubation bottles were transferred into the on deck incubation tubes covered by neutral density filters (Lee: Misty Blue [061] and Neutral Density Grey [210 ND]) which re-constructed the water-column light attenuation (55, 33, 14, 7, 4.5 and 1% incoming irradiance) and also removed red light. The incubation tubes were cooled by a constant flow of surface seawater mimicking sampling temperatures. All volumes were measured once the experiment ended to prevent excessive manipulation and potential iron contamination prior to the experiments.

Isotope additions

Nitrate and inorganic carbon

Dual-labelled ($^{15}NO_3$, ^{13}C-bicarbonate) light and dark nitrate (+^{13}C) and ammonium uptake (^{15}N-NH_4) incubations were performed in 2-l polycarbonate

bottles for approximately 24 hours. Stable isotope spikes (99.9% purity, CK Gas Products LTD, UK) of ^{15}N (0.1µmol $K^{15}NO_3$ / 100µl) and ^{13}C spikes (4.2507g sodium bicarbonate / 100ml Milli Q water) were introduced to both the light and dark bottles in order to achieve ^{15}N-NO_3 and ^{13}C enrichments of ~10% and ~4% respectively with respect to ambient nitrate and dissolved inorganic carbon (DIC) concentrations. All spikes were made up in almost completely iron free Mili-Q water of 0.040 nmol Fe, thus minimising iron contamination (~0.008 pmol Fe) to the incubation bottles.

Ammonium uptake and regeneration

To measure $^{15}NH_4^+$ uptake, the NH_4^+ incubation bottle was spiked with 0.1µmol $^{15}NH_4Cl$ / 100µl to also achieve an enrichment of ~10% with respect to ambient NH_4^+concentrations. To correct for $^{14}NH_4^+$ re-cycling by microzooplankton in the $^{15}NH_4^+$ incubation bottles (Gilbert et al., 1982b), exactly1-l was immediately drawn from the bottle to measure time zero NH_4^+ regeneration concentrations (Ro). This was achieved by filtering the 1-l through a 25mm (ashed) Whatman GF/F filter to remove particulates in order to collect a 900ml filtrate sample for ammonium analyses. This 900ml sample was then transferred into 6 [one bottle for each light depth] x 1-l glass Schotte bottles. Exactly 200µl NH_4Cl solution (10µmol / ml) was introduced into each of these bottles to act as a 'carrier' prior to freezing the samples at -20°C. This sample provided the time zero for NH_4^+ regeneration concentration (R0). The GF/F filter from this sample was then retained and stored at -80°C for later HPLC analyses. The remaining 1-l was used for the $^{15}NH_4^+$ uptake incubation.

Termination of experiments

After a 24 hour incubation period, the $^{15}NO_3$ (+^{13}C) incubations were filtered onto 25-mm ashed GF/F filters that were then stored frozen at -20°C prior to later measurements of ^{15}N and ^{13}C enrichment by stable isotope mass spectrometry at NOC. For the $^{15}NH_4^+$ incubations, the 1-l samples were filtered onto 25-mm ashed GF/F filters and for each bottle filtered, 900ml filtrate was recovered to measure ^{15}N isotopic dilution by regenerated $^{14}NH_4^+$

(Rt), exactly as for the Ro sample. Again 'carrier' was added (200µl) to the 900 ml filtrate and the sample was frozen as previously.

Recovery of aqueous $^{15}NH_4^+$ and $^{14}NH_4^+$ from the Ro and Rt bottles.

The aqueous NH_4^+ was recovered onto GF/F filters by diffusion (see Probyn, 1987) and the isotopic composition (and dilution) was measured by mass spectrometry as before. The diffusion recovery method entails adding sufficient MgO (± 1 teaspoon powder) to the Ro and Rt bottles which are then tightly sealed. This raises the aqueous pH to above 9 whereapon the NH_4^+ diffuses into the head-space over a 2-3 week period as ammonia. A 25mm GF/F filter suspended in the head-space from the lid is wetted with 50µl HCL, which recovers the ammonia as ammonium chloride (NH_4Cl). This filter is then dried (@ ~40°C overnight) and the isotopic composition (^{15}N:^{14}N) is measured by mass spectrometry as before.

Mass spectrometry and uptake calculations

All ^{15}N samples were run at the NOC's Stable Isotope Ratio Mass Spectrometry facility (NOC's-SIRMS) using a Eurovector elemental analyser coupled to a GV Isoprime mass spectrometer. The calibration standard was tyrosine certified by the International Atomic Energy Agency.

Nitrate and ammonium uptake rates were calculated according to the equations of Dugdale and Goering (1967) and Dugdale and Wilkerson (1986) and expressed as rates per day:

$$\rho NO_3 \text{ or } \rho NH_4 = (PE \times PN)/(Ro \times T)$$

where PE = percent ^{15}N enrichment of the PON fraction in excess of the natural abundance; PN = particulate N concentration ($\mu mol.l^{-1}$); T = experimental duration (hours) and Ro is the calculated aqueous ^{15}N enrichment at time zero.

Ammonium uptake was calculated according to Glibert et al., (1982a) that includes a correction for isotopic dilution from $^{14}NH_4$ excretion:

$\rho NH4 = (PE \times PN)/(R \times T)$

where R = exponential average enrichment:

$$R = Ro/kt(1-e^{-kt})$$

and:

$$k = (-\ln Rt/Ro)/T$$

where Ro and Rt are the measured aqueous ^{15}N enrichments at the beginning and end of an experiment.

Ambient Nutrient Measurements

Ammonium was measured at sea (by Achterberg, NOC) using the orthophthaldialdehyde (OPA) fluoresence protocol of (Holmes et al., (1999). Nitrate measurements were determined on-board (by Sanders, Stinchcombe; NOC) using standard cadmium (Cd) column reduction and colorimetric techniques on a Skalar San plus autoanalyser (Sanders et al., 2007).

Chlorophyll Measurements

Chlorophyll concentrations were measured on a Turner designs fluorometer following the Welschmeyer (1994) protocol after extraction in 90% acetone for 24 h in a dark refrigerator.

Results

In the results section, the hydrographic setting is first described to provide context for the nitrogen uptake data and results.

Hydrography

Temperature and salinity which one?

In the plots below (Fig. 1), note that pressure (bar) represents depth (m).

Figures 1(a-j)

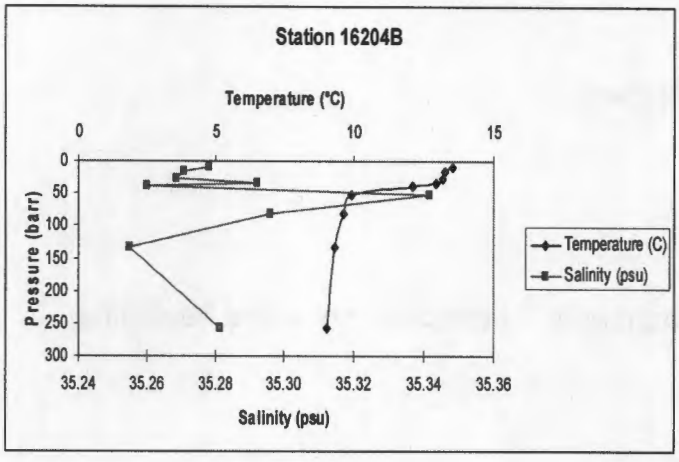

Figure 1a

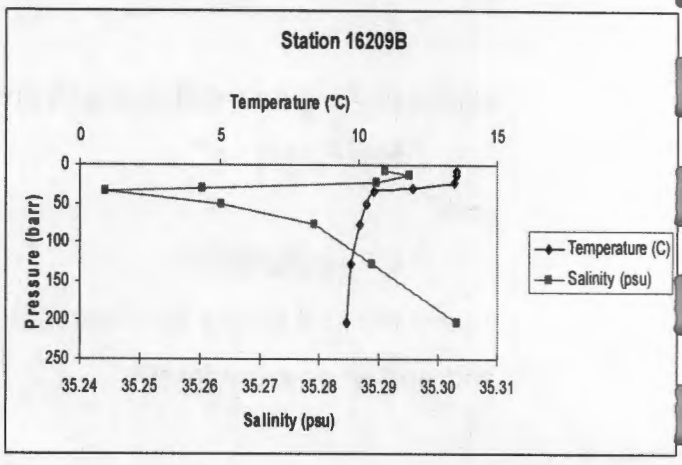

Figure 1b

Temperature profiles for stations 16204B and 16209B are very similar. Temperatures in surface waters are 13.52°C and 13.54°C for station 16204B and 16209B respectively, but decline gently from about 22m and 33m (figure 1a and 1b respectively) before rapidly declining between 33-35m, before remaining fairly constant throughout the rest of the water column.

Surface water salinity values in figure 1a are initially low (35.27psu) (compared to those in figure 1b) and further decrease down to ~25m before rapidly increasing to reach 35.29psu at 33m. There is then another rapid decline followed by a substantial increase to 35.34psu at 52m, after which salinity continues to decrease through the water column up to 130m before rising again. The salinity profile in figure 1b is much simpler, starting relatively higher than that at the previous station (35.29psu) and then declining through the water column up to 34m before psu starts to increase again.

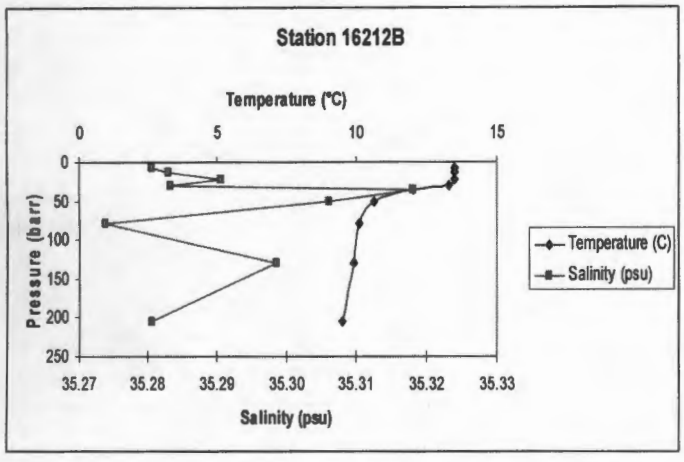

Figure 1c

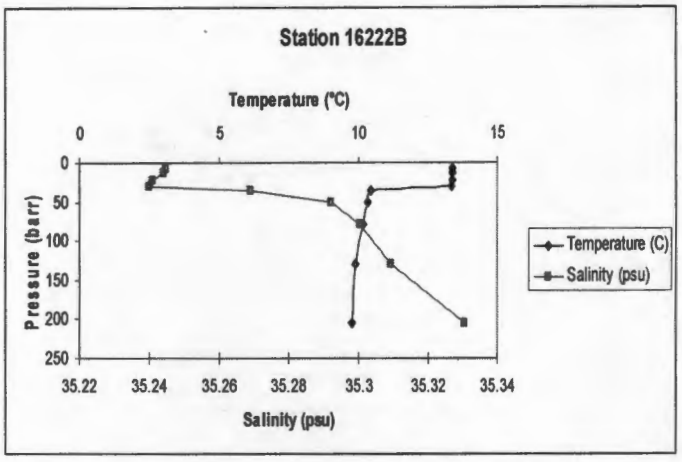

Figure 1d

Temperature profiles for the above two stations are again fairly similar with surface water temperatures ranging between 13°C and 14°C and remaining relatively constant down to 33 and 23m at station 16212B and 16222B respectively whereupon temperatures drop to approximately 10°C at 50m depth. After this point temperatures remain fairly constant throughout the rest of the water column.

The salinity profile at station 16212B fluctuates constantly, ranging from a minimum of 35.27psu at 78m to a maximum of 35.32psu at 35m. Salinity is relatively low but increases in surface waters. At approximately 30m, salinity begins to increase rapidly only to drop again after 35m to its minimum value at this station. Salinity at station 16222B however displays a fairly simple profile. Salinity is relatively low at the surface and remains low for 30m after which it increases throughout the rest of the water column.

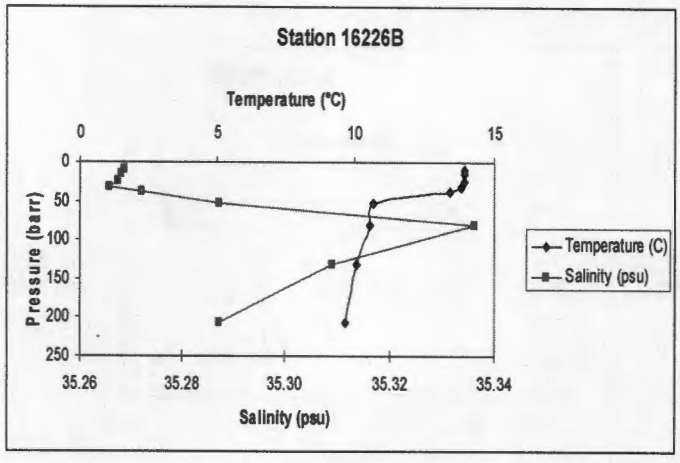

Figure 1e

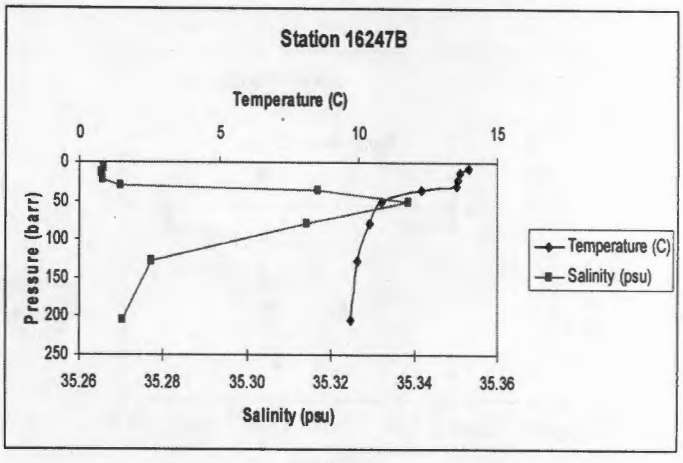

Figure 1f

Temperature profiles at these two stations (figure 1e-f) follow the same general pattern as for previous stations (figure 1a-d), with surface temperatures ranging between 13-14°C, remaining constant before declining at ~22m. After this point, temperature remains relatively constant, but on a slightly decline throughout the rest of the water column.

Salinity profiles are also similar, following the same pattern as before, where psu remains constant for first 20-30m and then sharply increases to 35.34psu at 80 and 50m respectively (e-f). Both stations then experience a decline in psu through the rest of the water column.

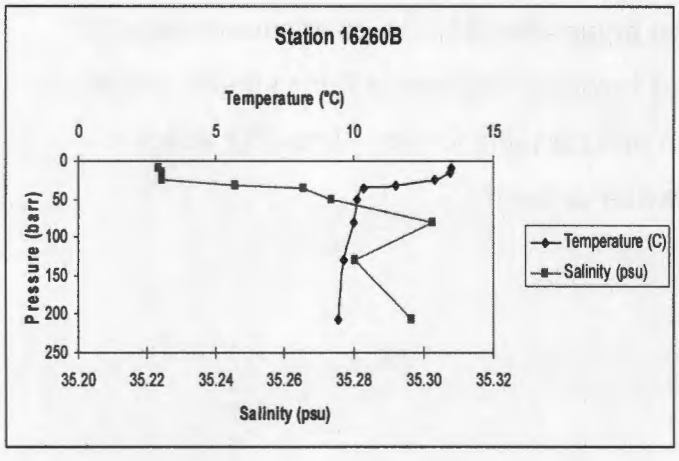

Figure 1g

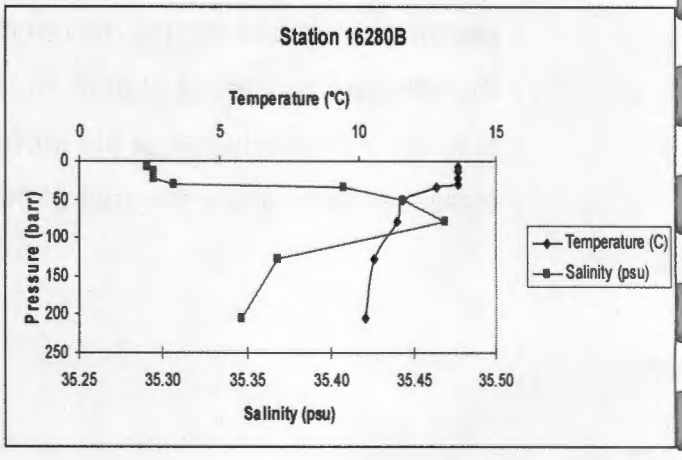

Figure 1h

At these two stations (figure 1g, h) temperature profiles are very similar to all the previous stations described. Salinity profiles at these two stations follow the same pattern as seen in figures d, e & f, being low in surface waters and increasing steadily with depth at both stations. Salinity values peak at 35.30psu at 80m at station 16260B and at 35.47 at 78m at station 16289B. Salinity then declines for another 50m or so at station 16260B and then increases again, while station 16280B continues to decline. In summary, there is fresher water at the surface, followed by a salinity maximum between 50-100m, followed by fresher water below this depth.

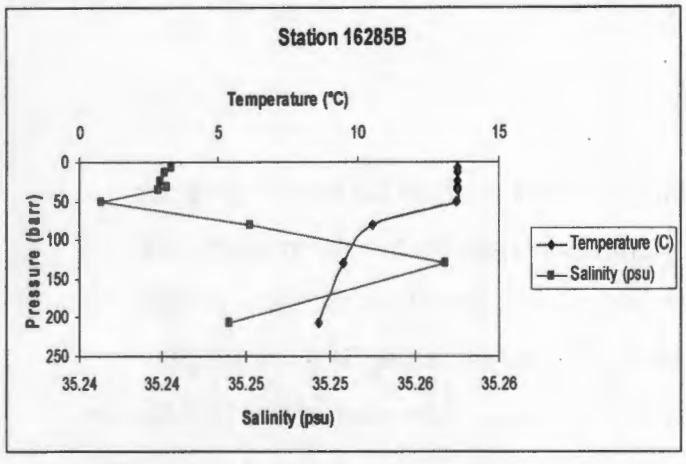

Figure 1i

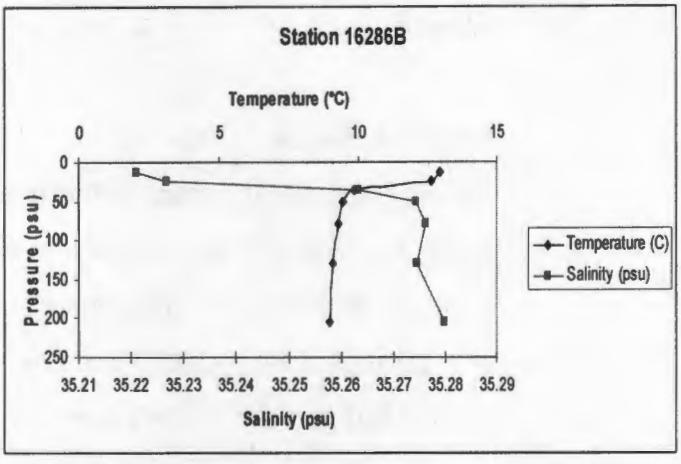

Figure 1j

At station 16285B (figure 1i) temperatures remain constant (~13°C) for approximately 50m before declining throughout the rest of the water column. Surface temperatures at Station 16286B on the other hand begin to decline at ~25m and by ~ 50m, temperatures (<10°C) remain fairly constant, declining slowly through the rest of the water column.

As before, surface Salinity is low initially at both stations, before rising to a salinity maximum between 50-150m, thereafter declining again with the presence of fresher water. Station 16285B's surface salinity values are low and continue to decrease until approximately 50m after which they again increase up to 130m and then again decrease. At station 16286B the salinity

profile is much simpler. Salinity increases through the water column almost constantly to reach a maximum of 35.28psu at 205m.

In summary, the general trend for all 10 stations is that the water column is quite strongly stratified, marked by surface waters of ~13-13.5°C and a thermocline at ~25-50m, below which water temperatures are typically below 10°C. Surface salinity associated with the warm surface water is typically low (~35.2 psu), but there is a sub-surface salinity maximum of ~35.3, before the underlying water freshens again. It should however be stressed that all salinities >35.2 can be regarded as being relatively high and what is evident are salinity differences at the 'salty' end of the scale. Both warm waters and salty waters are characteristic of summer conditions for this region of the N. Atlantic.

Nutrient Fields

As will become apparent in the following nutrient profiles for the 10 stations being considered, surface nitrate concentrations above the thermocline are almost universally < 5μM, while Si concentrations are close to 1μM or less, with phosphate concentrations being almost undetectable. Such nutrient concentrations are to be expected in mid-summer in this part of the N. Atlantic where summer stratification precludes the advection of nutrient rich water into the surface layer.

Figure (2a-j)

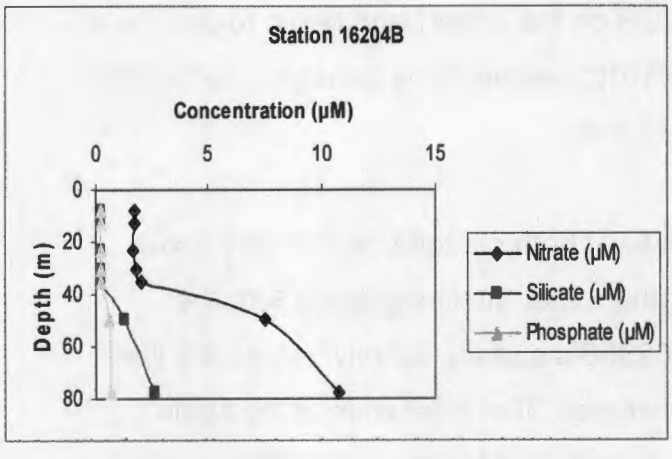

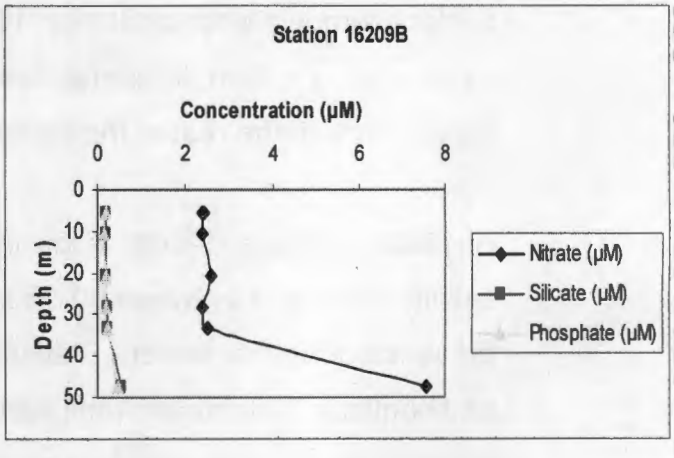

Figure 2a

Figure 2b

In detail, surface nitrate concentration at stations 16204B and 16209B remain relatively constant through the water column down to 35m and 33m respectively, after this point concentration increases sharply. At both stations, silicate and phosphate concentrations appear similar to each other. In figure 2a, concentrations of both silicate and phosphate are constant down to 35m, and in figure 2b they are constant down to approximately 33m. So at both stations nutrient concentrations remain fairly constant through the water column down to 33-35m where concentrations increase – even if only marginally in the case of silicate and phosphate.

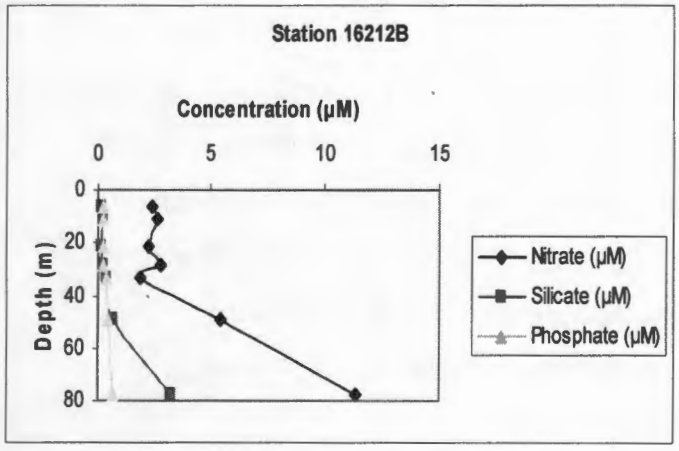

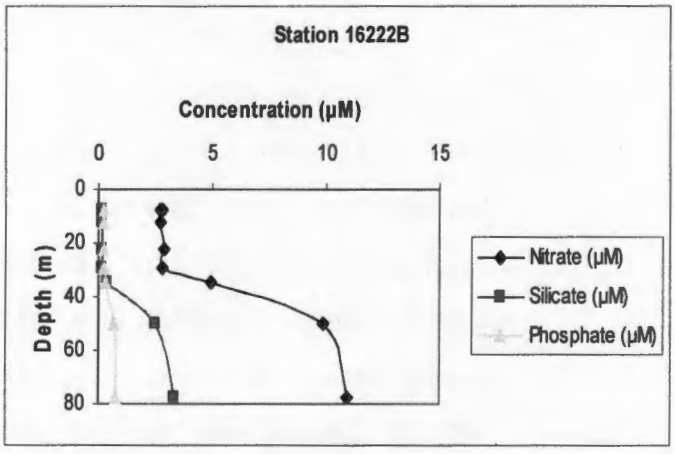

Figure 2c

Figure 2d

At these next two stations, surface nutrient concentrations remain relatively constant through the water column. However, at 33m and 29m (figure 2c and 2d respectively), concentrations of nitrate, silicate and phosphate increase. Nitrate concentrations increase sharply, silicate concentrations also increase sharply but to a lesser degree to nitrate and phosphate concentrations only increase slightly.

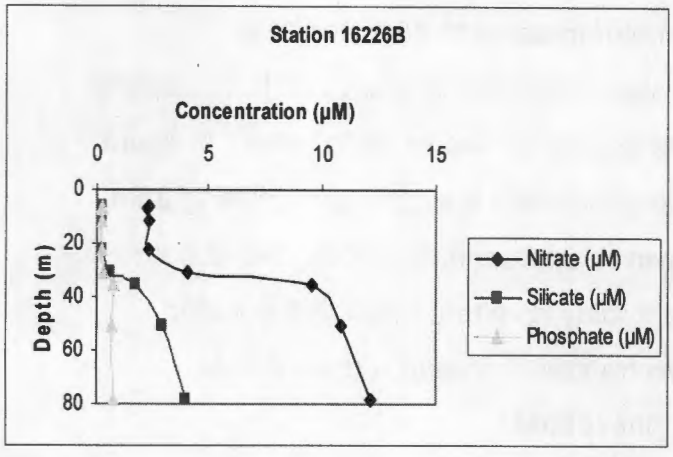

Figure 2e

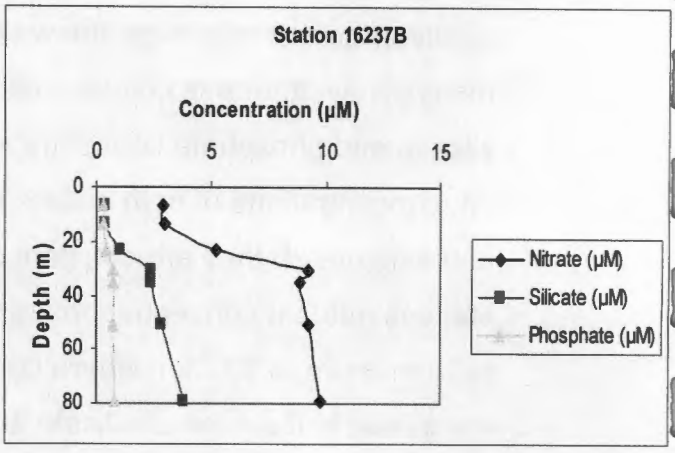

Figure 2f

As before, Station 16226B shows nutrient concentrations that follow a similar pattern to previous stations – surface concentrations are low (nitrate ~2.5µM; Si and PO_4 <<1µM) down to 30m, but then increase below the thermocline to varying degrees with nitrate concentration increasing the most (to ~10µM), then silicate (to ~3-4µM) and finally phosphate (to ~0.5µM). Nutrient concentrations for Station 16237B show almost exactly the same trends, although the nutricline is rather shallower.

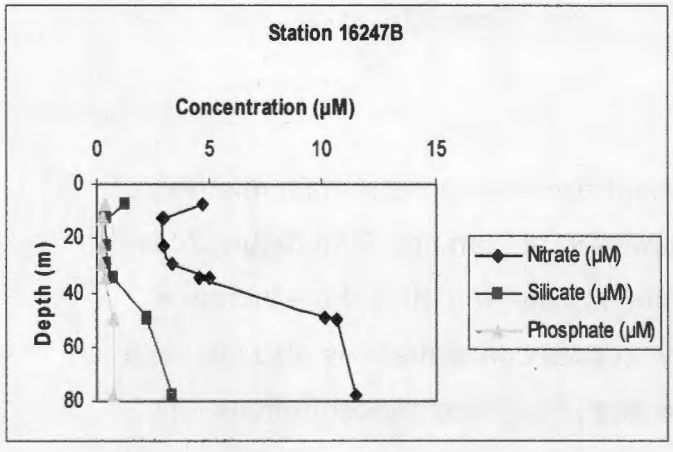

Figure 2g

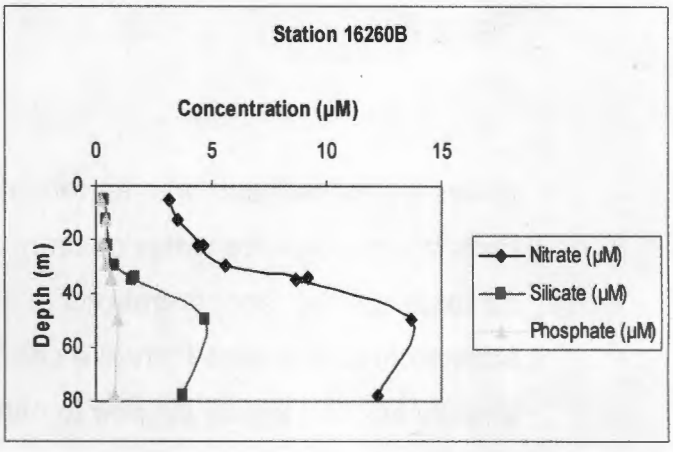

Figure 2h

Once again, surface and deep water nutrient concentrations for Stations 16247B and 16260B show almost exactly the same trends as for previous stations, with the exception being Station 16247B where there is a nutrient concentration minimum at ~20m, with slightly higher (but still low) surface nutrient concentrations.

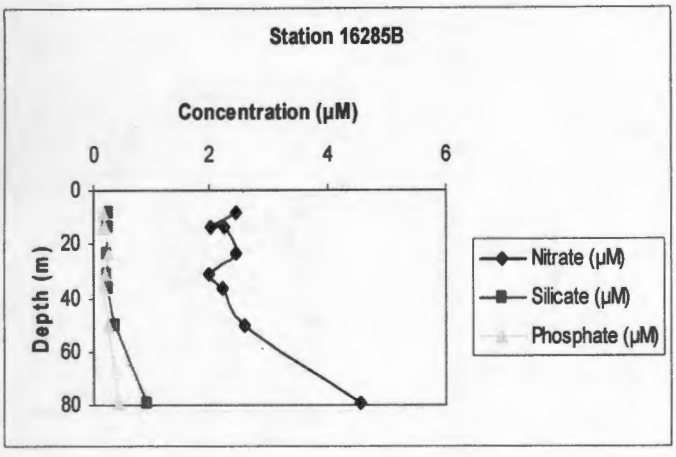

Figure 2i

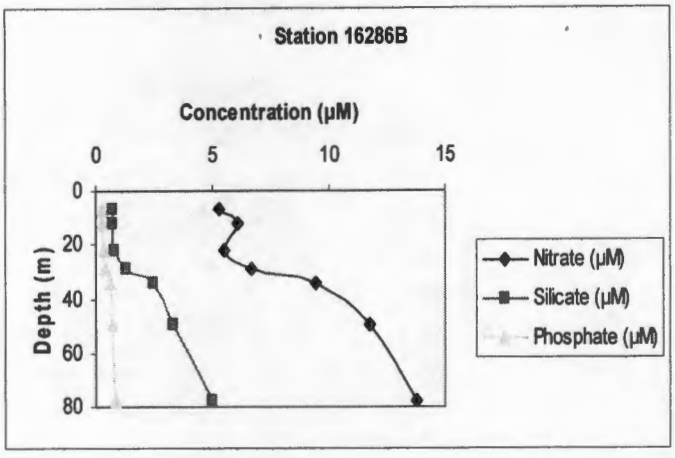

Figure 2j

Yet again, the nutrient profiles for surface waters at Stations 16285B and at 16286B show the same overall trends as for previous stations, with surface depletion and increases below the thermocline. However, nitrate concentrations in surface waters of Station 16285B are about 50% of those from other stations examined.

In summary, surface nitrate concentrations above the thermocline are universally low and less than ~5µM, with almost undetectable concentrations of Si and PO_4. Below the thermocline, however, Si and nitrate concentrations all rise, as is to be expected.

Phytoplankton

Phytoplankton biomass as chlorophyll a

a) Profiles

Phytoplankton biomass for the study region is expressed as chlorophyll a pigment (hereafter chl-a) for the intact, un-fractionated community and is

shown as profiles in Figure 3 (a-f). For all stations, chl-a concentrations in surface waters were generally very low, ranging from ~0.2µg l^{-1} to ~0.5µg l^{-1}.

Figures 3 (a-j)

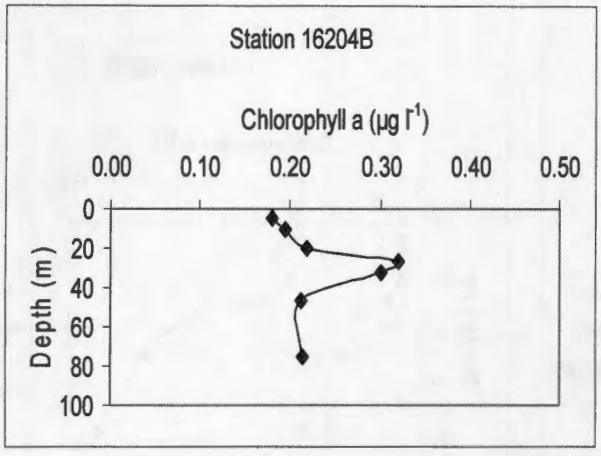

Figure 3a

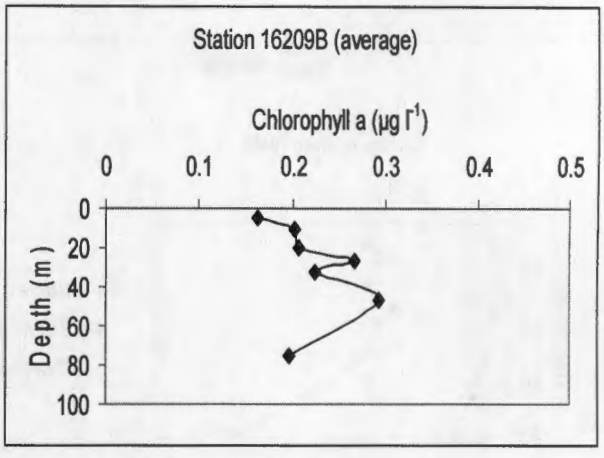

Figure 3b

In figure 3a, chl-a concentration is low at the surface (<0.2µg l^{-1}), but gradually increases with depth, reaching a maximum of 0.32µg l^{-1} at approximately 18m. Chl-a concentration then declines to about 0.2µg l^{-1} at ~42m through to ~80m. In figure 3b, chl-a concentration is once again low in surface waters (~0.15µg l^{-1}), but it increases gradually over the next 60m where it reaches a maximum of ~0.29µg l^{-1}, before declining again as before.

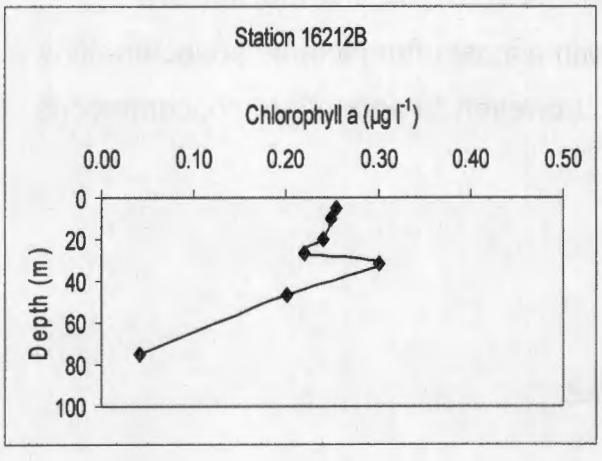

Figure 3c

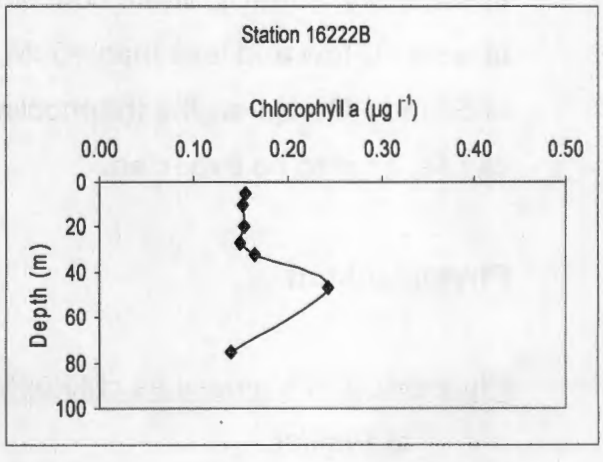

Figure 3d

In Figure 3c, surface chl-a concentration are again low (~0.25µg l^{-1}), but there is a subsurface maximum of 0.30µg l^{-1} at ~38m before chl-a concentration steadily declines through the rest of the water column. Similarly in figure 3d, chlorophyll values are low in the surface waters (~0.15µg l^{-1}) and remain constant for about 20m before increasing to a maximum of 0.24µg l^{-1} at approximately 42m. Below that, it gradually decreases.

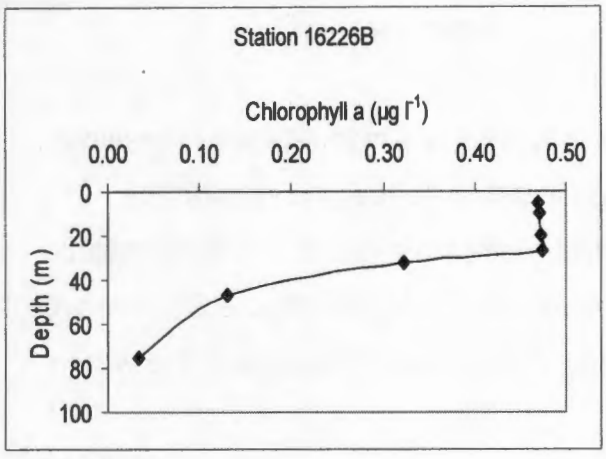

Figure 3e

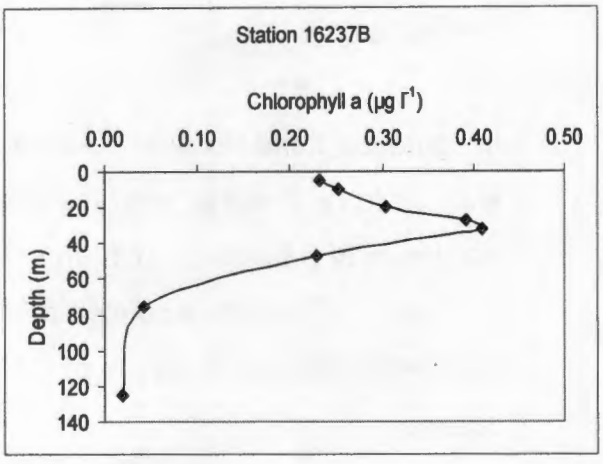

Figure 3f

Chlorophyll concentrations at this station (figure 3e) are about double those of previous stations, with a maximum surface value of 0.47µg l^{-1}, which extends down to ~35m. Below that depth, chlorophyll concentration decreases rapidly throughout the rest of the water column. However, in figure 3f chlorophyll concentration is marked by a pronounced subsurface maximum of 0.41µg l^{-1} at 38m, before it then declines towards zero at about 52m.

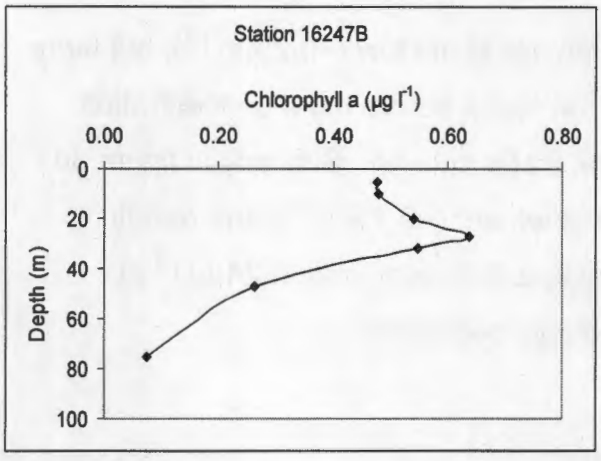

Figure 3g

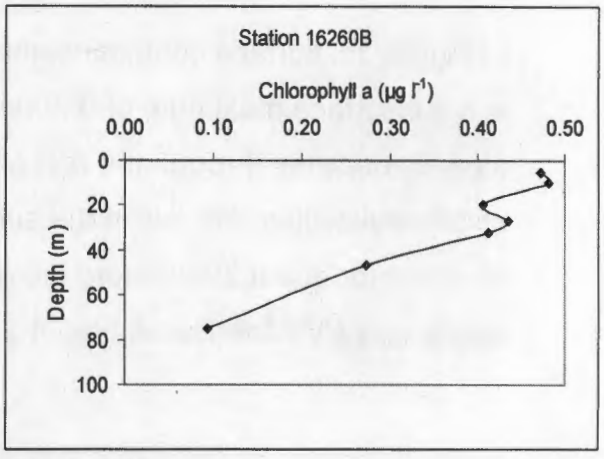

Figure 3h

In figure 3g, surface chlorophyll concentrations are high relative to previous stations (a-f). Even so, surface values increase to reach a subsurface maximum of 0.64µg l^{-1} (27m) from which point chl-a gently declines towards <0.1µg l^{-1}. Chlorophyll concentrations at station 16260B (figure 3h) however, fall from a surface maximum of 0.48µg l^{-1} and decline throughout the water column.

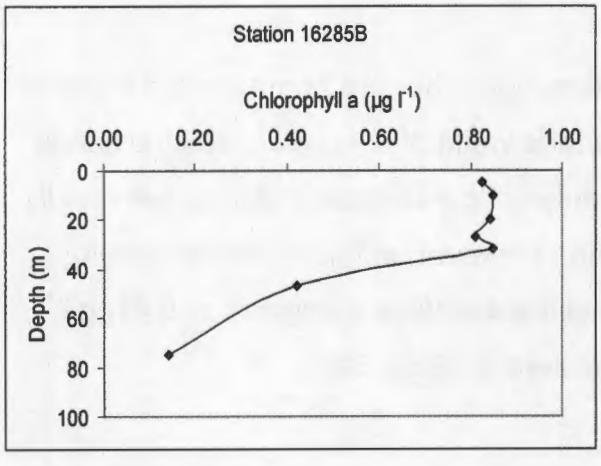

Figure 3i

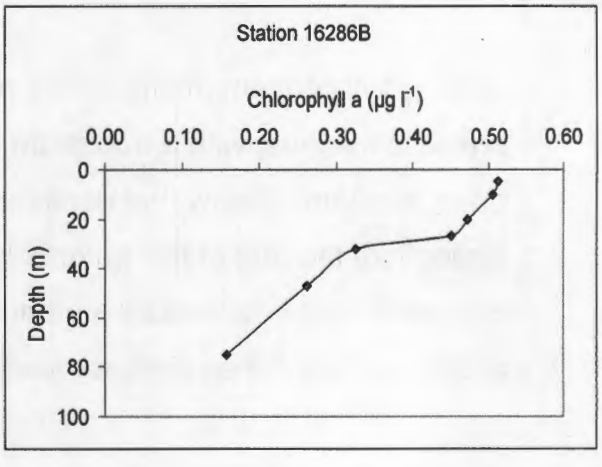

Figure 3j

Station 16285B exhibits the highest maximum chlorophyll concentration of all the stations. The subsurface maximum falls at 32m with a value of 0.85µg l^{-1}. Before this depth, concentrations were fairly constant, however below 32m concentrations decline steadily. In figure 3j, maximum chlorophyll

concentrations fall within range of the previous stations (bar figure 3i and 3g) and show the same general trends of a sharp decline below the thermocline.

b) Integrated chlorophyll-a

A comparison of phytoplankton biomass for different stations in a region is best achieved by integrating biomass over the euphotic depth, rendering stations comparable in terms of potential food available, for example. Water column phytoplankton biomass is therefore expressed as a histogram of integrated chl-a biomass for the euphotic zone (mg chl-a m^{-2}) in Figure 4.

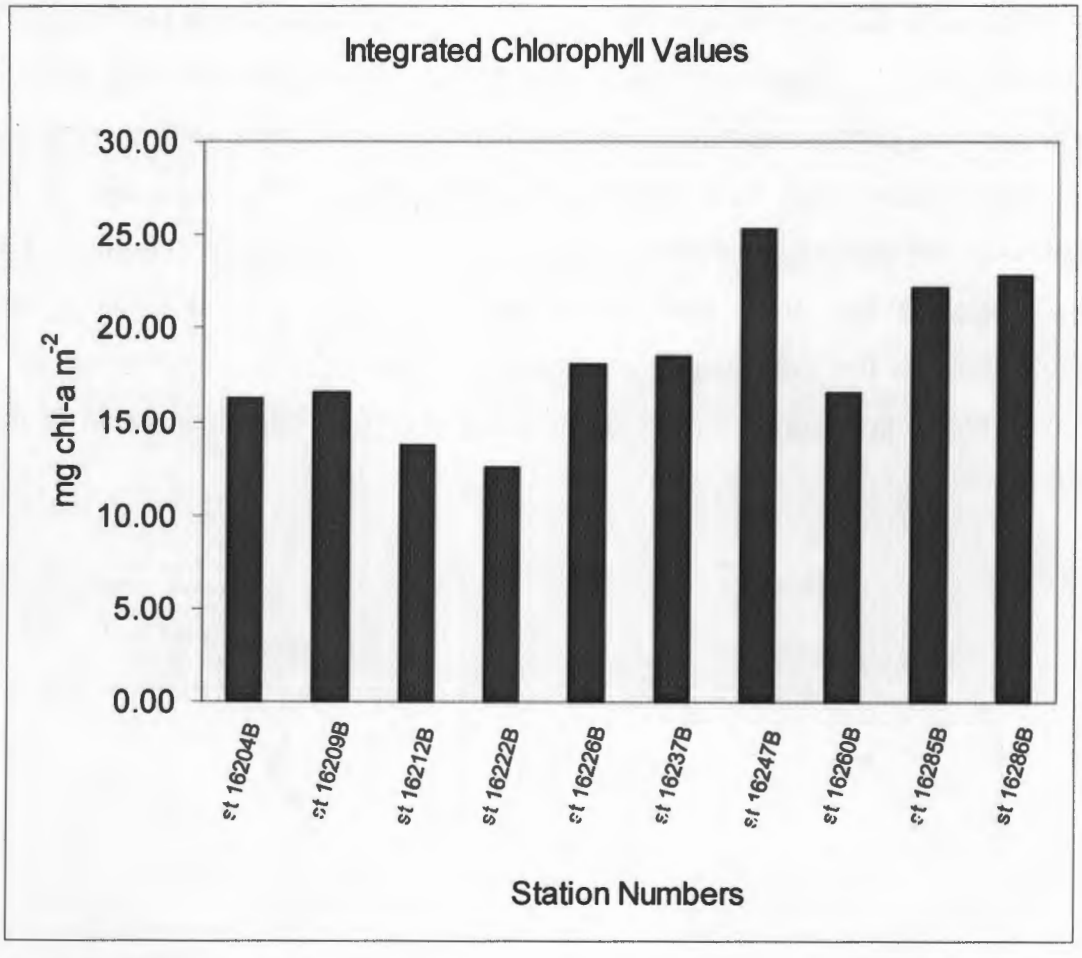

Figure 4: Integrated chlorophyll concentration values (mg chl-a m^{-2}) for all stations in the sample area

Overall, there is a general mean integrated chl-a value of ~15-20 mg m^{-2}, although some stations exceed this value. Station 16247B for example has the largest integrated chlorophyll value (25.39mg m^{-2}) closely followed by

stations 16286B and 16285B (22.88 and 22.15mg m^{-2} respectively). Station 16222B exhibits the lowest value of (12.55 mg m^{-2}).

Nitrogen uptake rates

1. Depth profiles of N15 uptake.

Profiles of nitrogen uptake, differentiated between 'new' production (nitrate uptake; ρNO_3) and 'regenerated' production (ammonium uptake; ρNH_4) are shown in Figures 5(a-h). Nitrate uptake is further differentiated into that measured in the light (ρNO_3 L) and that measured in dark bottles where light is excluded (ρNO_3 D). What is common to all the profiles (below) is that ρNH_4 exceeds ρNO_3 L, which in turn exceeds ρNO_3 D. This implies that the nitrogen requirements of the community are largely based on regenerated or re-cycled nitrogen, rather than new nitrogen. Furthermore, ρNO_3D appears to be relatively unimportant, at least in surface waters. Another general feature of all the profiles is that ρN is highest in near-surface waters, and declines with depth through the euphotic layer. However, most profiles are marked by a sub-surface maximum in ρN. A detailed presentation and description of the results follows:-

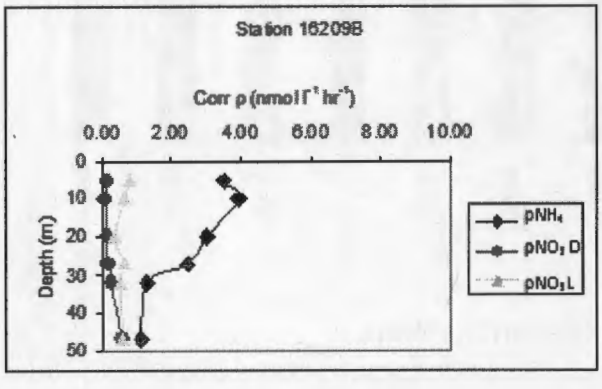

Figure 5a

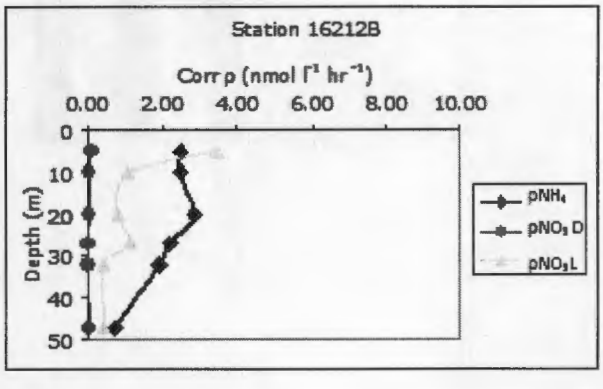

Figure 5b

For stations 16209B and 16212B, ρNH_4 is initially relatively low (~3.8nmol l^{-1} h^{-1}) in surface waters (5m) at station 16209B, but increases slightly to reach this stations' maximum uptake rate (~4.0nmol l^{-1} h^{-1}) at 10m, which

corresponds to the 50% ambient light depth. Below this, ρNH_4 gently decreases through the water column. At around 30m, NH_4 uptake becomes constant, but is at its lowest. Nitrate uptake in the light (ρNO_3 L) is rather low in surface waters (<1.0nmol l^{-1} h^{-1}; about 25% of ρNH_4) and in fact remains relatively constant throughout the water column to ~45m depth. Dark nitrate uptake (ρNO_3D) is very low (~0) in the first ~10m, after which there is a slight increase in uptake values at the base of the euphotic layer.

As before (station 16222B, see figure 5b), ρNH_4 dominates ρN overall, except at the surface where ρNO_3 L (~3.8nmol l^{-1} h^{-1}) exceeds ρNH_4 (~2.5nmol l^{-1} h^{-1}). Below this, however, ρNO_3 L remains low (~2nmol l^{-1} h^{-1}) throughout the water column. Ammonium uptake reaches its maximum rate (~3nmol l^{-1} h^{-1}) at a depth of 20m. From this point on, NH_4 uptake decreases steadily with depth. Dark NO_3 uptake is very low (similar profile to station 16209B) and remains constant throughout the water column.

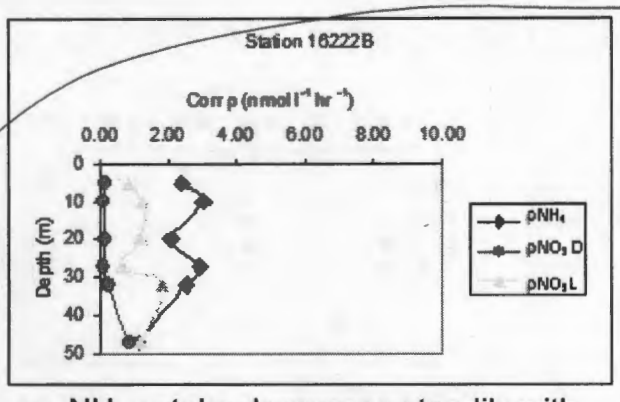

Figure 5c

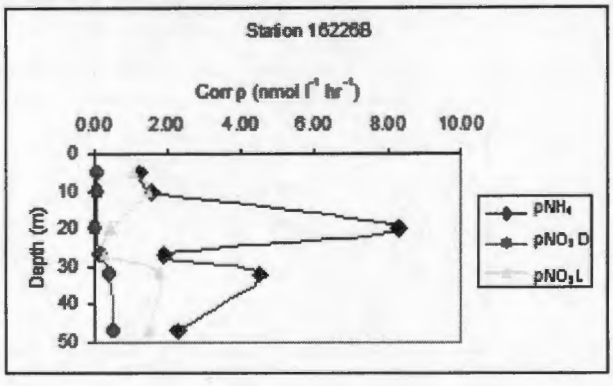

Figure 5d

Once again, NH_4 uptake dominates total N uptake, but it exhibits some variability between ~2-3nmol l^{-1} h^{-1} over the top 30m, before declining towards 1nmol l^{-1} h^{-1} by about 48m. Light NO_3 uptake shows similar variability around 1nmol l^{-1} h^{-1}, and at approximately 45m it exceeds the NH_4 uptake rate slightly. Dark NO_3 uptake remains constant from 5m to ~30m, but after 30m the rate increases steadily to nearly 1nmol l^{-1} h^{-1}, almost exactly the same as ρNO_3 L.

At station 16226B, NH_4 uptake remains constant for ~5m and then exponentially increases down to 20m to reach a maximum of 8.32nmol l^{-1} h^{-1}, it then similarly decreases down to approximately 28m, contrasting sharply with the previous station. The NH_4 uptake rate then increases sharply for approximately 5m after which it again decreases. Surface light NO_3 uptake begins low; and for the first 5m is balanced with NH_4 uptake, however after 10m ρNO_3 L begins to decline sharply to 28m, from which point there is a gentle increase to 32m, after which uptake values decrease/remain constant. Dark NO_3 uptake remains consistently low down to approximately 28m, where there is a noticeable increase in uptake values, after which uptake again stays constant.

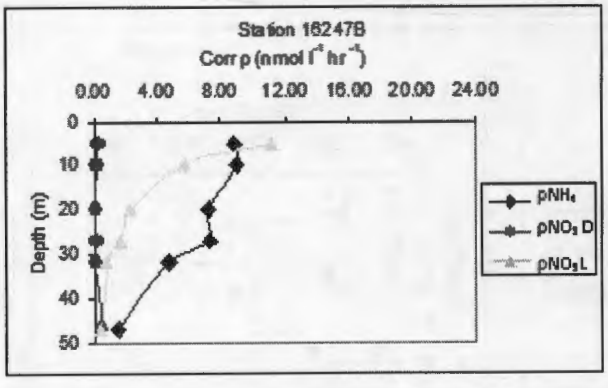

Figure 5e

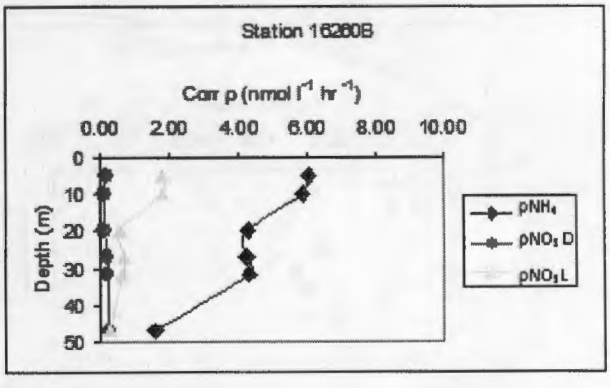

Figure 5f

For station 16247B, NH_4 uptake (~9nmol l^{-1} h^{-1}) is constant over the first 10m, but then gradually decreases for another 10m. At 20m depth, rates remain constant for ~12m and then again decline through the rest of the water column. The light NO_3 uptake profile follows a similar pattern to the previous station; it is initially very high (exceeding NH_4 uptake at a rate of 11.17nmol l^{-1} h^{-1} at 5m) but from 5m to approximately 28m, the uptake rate declines. At ~30m, uptake is constant throughout the rest of the water column. Dark NO_3 uptake remains at the same low rate throughout the water column with a very slight increase after 30m.

For station 16280B, NH_4 uptake starts quite high and remains relatively constant for 5m. It then declines until 20m depth, and once again remains constant until 28m depth and after which it gradually declines again. Light NO_3 uptake starts relatively low, remains constant for 5m and then gently declines – this profile follows the same pattern as NH_4 uptake at the same station – however, the decline after 28m is very slight. Dark NO_3 uptake rates remains low and constant throughout the water column with a slight increase at approximately 35m.

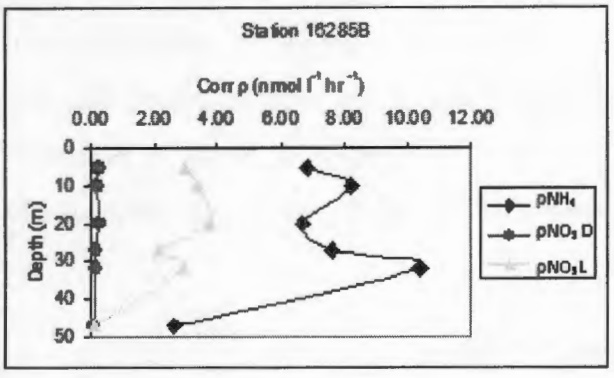

Figure 5g

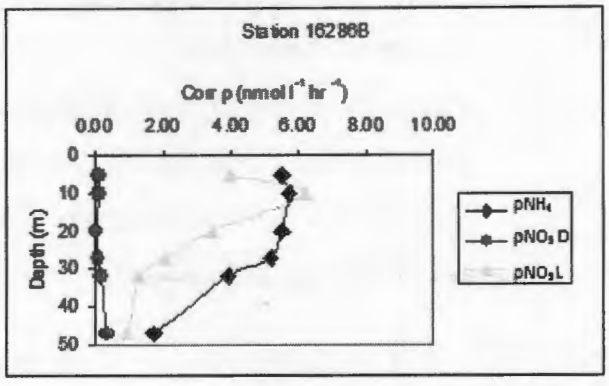

Figure 5h

For station 16285B, NH_4 uptake is high (~7nmol l^{-1} h^{-1}) initially and then increases for a further 5m. Uptake rates then decline again, but increase after 20m depth to reach a maximum of 10.38nmol l^{-1} h^{-1} by 32m. This Station has the highest NH_4 uptake rates of all the stations sampled. NO_3 (dark) uptake is low and constant throughout the water column. NO_3 (light) uptake is relatively high (~3nmol l^{-1} h^{-1}) in surface waters, but increases to reach a maximum (~4nmol l^{-1} h^{-1}) at 20m after which it declines for ~8m. After that point there is a slight increase for about 2m and then uptake values decline relatively sharply.

For station 16286B, NH_4 uptake rates in surface waters are relatively high, increasing very slightly for 5m and then declining very gently until ~28m. At 28m the rate of decline increases. Surface light NO_3 uptake starts relatively high (3.99nmol l^{-1} h^{-1}) increasing sharply until 10m depth where NO_3 uptake exceeds NH_4 uptake at a rate of 6.23nmol l^{-1} h^{-1}, after which there is a decline

for approximately 20m. After 30m depth uptake rates remain constant/decrease very slightly. Dark NO_3 uptake remains low (0.05 ~ 0.15nmol l^{-1} h^{-1}) and constant throughout most of the water column, with a slight increase at 30m.

2. Integrated nitrogen uptake rates

Integrated new production rates (mmol N m^{-2} h^{-1}) represents new production that is available to zooplankton consumers and/or for vertical export into the deep ocean at any station. Integrated ammonium uptake represents re-cycled nitrogen, as before. Integrated uptake rates for both nitrate and ammonium are presented in Figure 6.

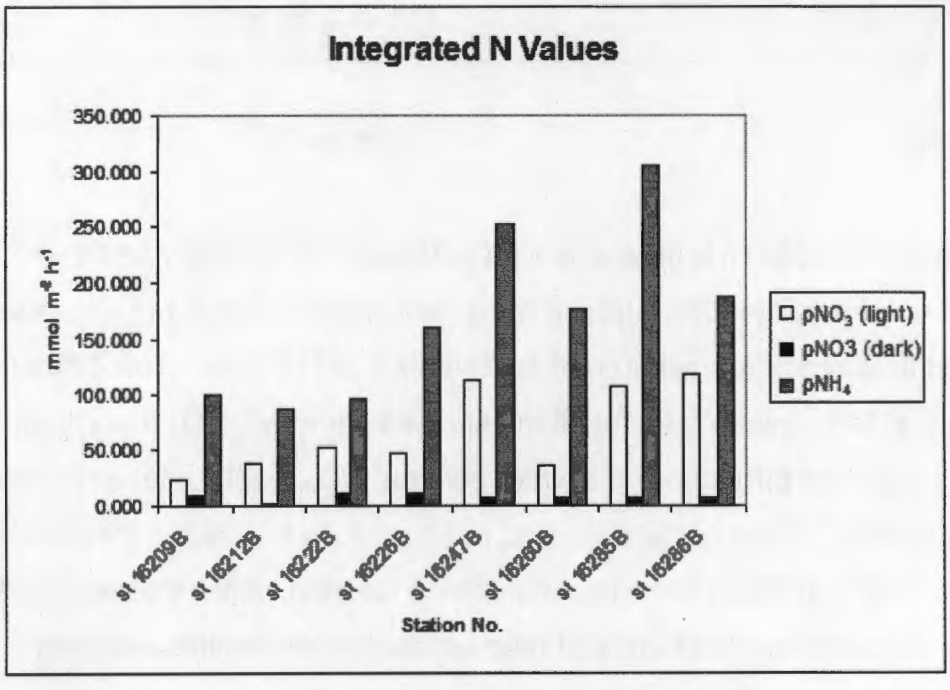

Figure 6: Integrated nitrogen (NO_3 (light), NO_3 (dark) and NH_4) uptake values (mmol m^{-2} h^{-1}) for all stations in the study region

This histogram shows overall (integrated) NH_4 and NO_3 uptake rates (light and dark) as mmol m^{-2} h^{-1} for each station. Integration allows for a more comprehensive assessment of relative new and regenerated production at each station in the study region. Everywhere, the data clearly demonstrate the

overall significance of regenerated NH_4^+ as the primary nitrogenous resource for phytoplankton relative to the contribution by nitrate. Dark nitrate assimilation is unimportant. The highest light NO_3 integrated uptake value (Station 16286B) departed from the mean (67.40 mmol m^{-2} h^{-1}) by 176.7%, while the station with the lowest light uptake rate – station16209B – was 34.2% below the mean. Integrated ammonium uptake on the other hand has a maximum rate (253.42mmol m^{-2} h^{-1}) that departs from the mean by 178.6% and a minimum rate (station 16222B) which is 47.2% below the mean.

As can be seen above, integrated dark NO_3 uptake values are all fairly similar and very low, as expected from the uptake profiles (Fig 2 a-h). Integrated dark nitrate uptake values at each station are very low; the percentage total nitrate uptake (light + dark) for which dark NO_3 uptake is responsible is 1.3%.

3. f-ratios

The relative importance of 'new' nitrate assimilation to 'regenerated' nitrogen assimilation is expressed as the f-ratio, as shown in Table 1, below.

Table 1:

Station	Depth	f-ratio (light + dark)	Average f-ratio
16209B	5	0.17	0.12 f < 0.5 regenerated
	10	0.12	
	20	0.07	
	27	0.15	
	32	0.18	
	45	0.01	
16212B	5	**0.58**	0.33 f < 0.5 regenerated
	10	0.30	
	20	0.21	
	27	0.34	
	32	0.18	
	45	0.36	

16222B	5 10 20 27 32 45	0.24 0.27 0.34 0.15 0.40 0.24	0.27 f < 0.5 regenerated
16226B	5 10 20 27 32 45	0.44 0.47 0.05 0.06 0.23 0.29	0.26 f < 0.5 regenerated
16247B	5 10 20 27 32 45	**0.55** 0.19 0.24 0.17 0.13 0.03	0.22 f < 0.5 regenerated
16260B	5 10 20 27 32 45	0.22 0.23 0.10 0.10 0.09 0.02	0.12 f < 0.5 regenerated
16285B	5 10 20 27 32 45	0.29 0.28 0.35 0.21 0.21 0.02	0.23 f < 0.5 regenerated
16286B	5 10 20	0.41 **0.52** 0.38	0.35 f < 0.5 regenerated

	27	0.28	
	32	0.23	
	45	0.26	

As can be seen in the above table, the values highlighted in bold are f-ratios >0.5; all these values fall in the surface euphotic zone. Values of 0.5 indicate that the balance between uptake rates for NH_4 and NO_3 are in balance (or very nearly in balance) (see station 16226B, at 20m and station 16247B, at 45m). The final column displays the average f-ratio values for the entire water column. All such f-ratios are <0.5 indicating that overall, regenerated production is dominant.

Station 16209B and16260B have the lowest f-ratios (0.12) and station 16286B has the highest (0.35), although this is still well below the 0.5 mark. Higher f-ratios consistently fall within the first 20m with few exceptions (station 16222B at 32m). F-ratios tend to decrease through the water column, with the lowest ratios falling at 32m/45m depth.

There is a general trend towards higher f-ratios occurring in the surface waters relative to deeper waters.

Table 2:

Station	**Integrated NH_4 Uptake**	**Total (light + dark) Integrated NO_3 Uptake**	**f-ratio**	**f-ratio**
	(mmol m^{-2} h^{-1})	**(mmol m^{-2} h^{-1})**	**(light + dark NO_3)**	**(light NO_3 only)**
16209B	100.44	32.75	0.12	0.19
16212B	86.63	39.62	0.33	*0.31*
16222B	97.24	64.32	0.27	0.35
16226B	158.99	59.03	0.26	*0.23*
16247B	358.62	121.51	0.22	0.24
16260B	175.54	44.29	0.12	0.17

16285B	304.4	114.92	0.23	0.26
16286B	186.94	125.90	0.35	0.39

As can be seen in the above Table 2, integrated NH_4 uptake rates far exceed total (light + dark) integrated NO_3 uptake rates at all stations. This is reflected in the f-ratios that are all below 0.5, indicating that the balance of N uptake is skewed towards NH_4 uptake, which accounts for between 66 and 88% of the total N demand by phytoplankton during summer.

In the final column, f-ratios have been calculated excluding the dark NO_3 uptake rates. It can be seen that while this leads to a general trend of increased f-ratio values (excluding f-ratios at station 16212B and 16226B, where the light only f-ratio is less than the light + dark ratio), it does not push any of the ratios above 0.5. It can therefore be safely assumed that leaving out the dark data will not lead to significant increases in f-ratios; unless the combined light + dark f-ratio value was already very close to 0.5.

Discussion

1.. Hydrography: temperature and salinity

Temperature profiles in the study region are all fairly similar, with surface temperatures of approximately 13-14°C throughout the euphotic zone. Thereafter a strong theremocline becomes apparent between 25-35m, as would be expected in the summer months. Below that, temperatures of the aphotic layer fall sharply to ~10°C, as would also be expected in summer stratified conditions. Station 16285B is the only station where the temperature profile differs slightly from the norm since temperatures remain isothermal to a depth of ~50m compared with 25-35m at the other stations. It is therefore clear that thermal stratification is occurring down to and between the depths of 25 and 50m as a result of summer sun-warming and in the absence of significant wind events that would otherwise mix the water column.

Salinity in the study area varies considerably at the different stations and also through the water column. Surface salinity falls into two approximate groups; stations' whose salinity at the surface ranges between ~35.22-35.24psu (Figures 3h, i, j) and stations whose surface salinity is slightly higher, falling between ~35.27-35.30psu (figures3a, b, c, e, f, h). Salinity does not fall beneath 35.20psu at any of the stations. Salinity in surface waters is generally lower than at intermediate depths (20-50m) where there is salinity spike (maximum or minimum). Interpretation of the salinity results requires a theoretical consideration of the processes that affect salinity – the balance between evaporation and precipitation. Thus regions of net evaporation will be characterised by higher salinity values, while regions that experience significant precipitation will be characterised by a freshening of surface waters. Values of salinity of >35.20 all exceed, for example, the salinity signature of newly upwelled Benguela water (~34.80 psu), so the salinity values of the N. Atlantic in summer can be considered to be fairly high, as one might expect in the summer where surface ocean warming leads to evaporation and therefore an increase in salinity especially in surface waters. Furthermore, given that in the northern hemisphere, surface currents flow in a north-easterly direction due to the Coriolis Effect, this will deliver warm salty water from the equator into the N. Atlantic basin, which compounds the general increase in salinity observed. However, the slight freshening of surface waters may welll be due to freshwater dilution from rainfall that is nevertheless a feature of northern temperate latitudes, even in summer.

2. <u>SST and Eddy di-pole</u>

The study region during the cruise was characterised by variable SST and an eddy-dipole, as can be seen from the image and diagram below.

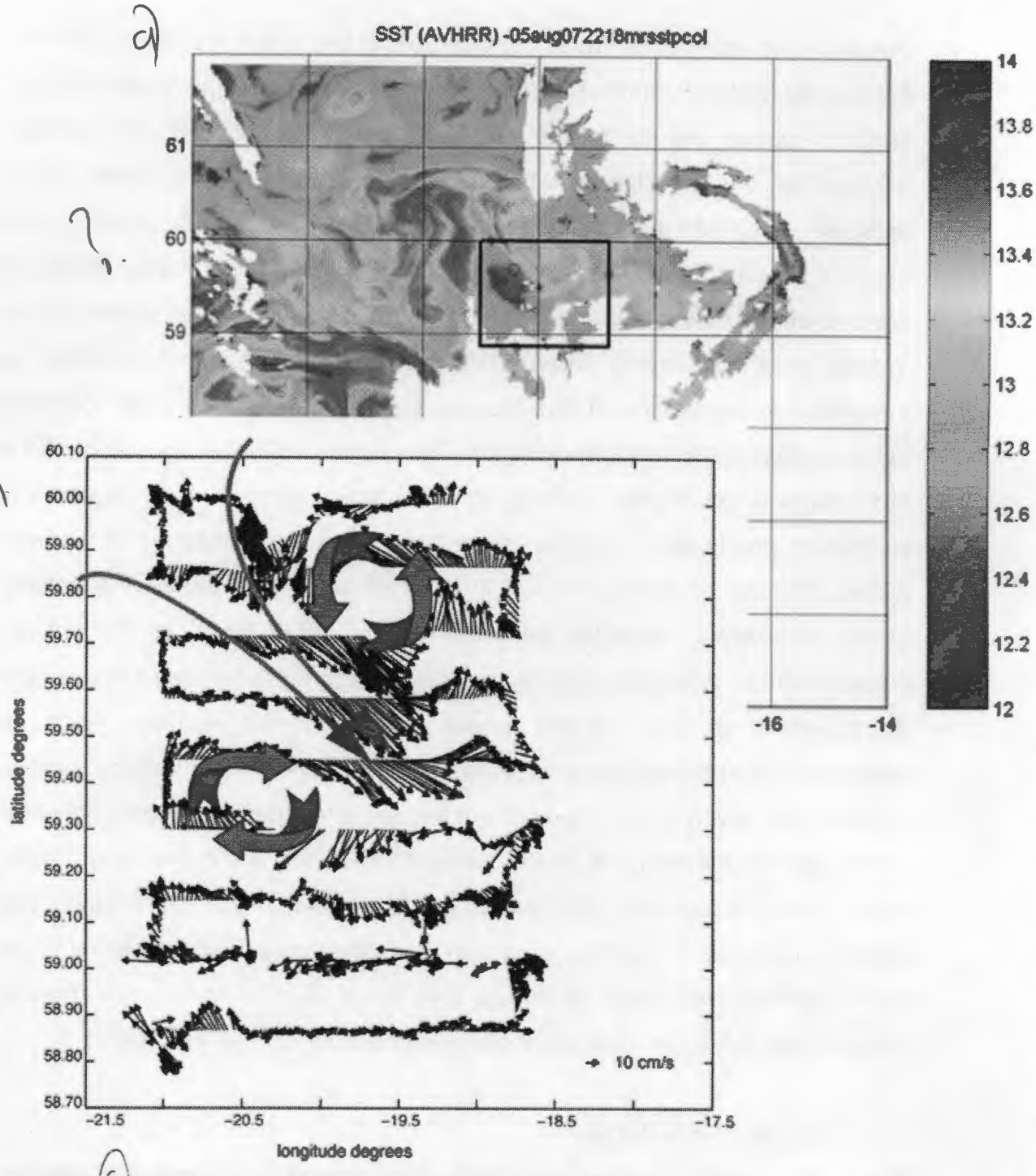

Figure 9: counter-rotating currents of the eddy dipole are clearly seen in the ocean currents (bottom) and also in their cold and warm surface signatures in the sea-surface temperature satellite image (note blue and bright yellow patches in black rectangle (top).

The figure above shows the variable SST of the study region and the position of the clockwise and anticlockwise eddy structures that were a feature of the study region. The small black arrows show the acoustic doppler current

profiles (ADCP) of current velocities for the region, where longer arrows represent stronger flows. What is apparent is that the south-easterly flow between the eddy dipole is rather strong and it can be seen in the SST image above (within the black box) as a streak of higher temperatures between a cold clockwise eddy to the south-west and a warmer anticlockwise eddy to the northwest. All of these features significantly alter the delivery of nutrients to surface waters and indeed, the filament between the eddies is marked by elevated chl-a concentrations (data not shown) that also results in higher rates of overall productivity.

3. Nutrient Fields

Nutrient concentrations across the board were low and constant in surface waters to a depth of approximately 30m; after which nutrient concentrations began to increase below the thermocline. Thus, there is a strong nutricline at the majority of the stations in the study region which corresponds to the thermocline (see figures 3a – j) which is to be expected. In the upper layers – where nutrient concentrations are low – nutrients have been depleted from the water column because of assimilation by phytoplankton in the region. As one moves down, deeper through the water column and phytoplankton become light limited and their biomass becomes reduced, nutrient concentrations are able to again increase.

Silicate concentrations are all fairly low in surface waters (<1μM), with the exception of station 16247B which has a relatively higher surface silicate concentration of 1.27μM. Low silicate concentrations are widely thought to limit diatom growth, especially in larger cells (Nelson and Tréguer, 1992 in Lucas et al. 2007). This coupled with low nitrate and phosphate concentrations in surface waters down to 30m, strongly suggests that the spring diatom-dominated phytoplankton community structure is likely to have been replaced by one dominated by smaller celled phytoflagelllates that don't require Si and furthermore, are able to scavenge nutrients at low nutrient concentrations and in a low-light environment (Lucas et al. 2007).

4. Chlorophyll-a biomass

During the summer (2007) of this study, phytoplankton biomass (chl-a concentration) was relatively low (~0.20µg l^{-1}) in the immediate surface waters (0-25m) at half of the stations (station 16204B, 16209B, 16212B, 16222B, 16237B). The rest of the stations had chl-a concentrations of approximately 0.5 µg l^{-1} in the surface waters, these stations included station 16226B 16247B, 16260B, 16285B and 16286 (See figure 5a-i), particularly at the end of the study period. At all stations however, there is evidence for a sub-surface chl-a maximum associated with the 50 or 25% light depths (30m) (exceptions include station 16260B and 16286B). Below that (~25-35m), chl-a concentrations declined with depth. The decline in chl-a biomass below ~30m at most stations illustrates how phytoplankton biomass becomes light limited despite an increase in nutrient concentration at most stations. This suggests an inverse relationship between nutrient concentration and chl-a biomass; however one would expect to see a time lag in increasing biomass and decreasing nutrient concentration (see figure 4a-i). Furthermore, the establishment of a sub-surface chl-a maximum reflects the migration of cells down the water column towards the nutricline to take advantage of small amounts of nutrients diffusing across the thermocline (Anderson & Lucas, 2007). These smaller cells would be able to outcompete the larger cells at low nutrient concentrations because of a higher surface area to volume ratio (A/v). One consequence of this downward shift in the water column is that phytoplankton will experience reduced light availability (as has already been mentioned) (Brown and Hutchings, 1985) - although this can be compensated by physiological adaptations to lower light as reflected by changes in P vs. E characteristics. Clearly, however, a shift in phytoplankton community structure from diatoms to smaller cells will affect the efficiency of the 'biological pump' as well as affect the ecosystem's ability to support commercially important fisheries such as the Cod fishery (Anderson & Lucas, 2008).

Station 16247B, 16286B and 16285B have the highest integrated chlorophyll-a values (25.39mg m^{-2}, 22.88 mg m^{-2} and 22.15mg m^{-2} respectively) (see figure 6). These stations correspond to the three stations with the highest integrated nitrate and ammonium (light) values (see figure 6).

Another important point to consider if a shift in community structure should occur, is that while being smaller (to maximise nutrient uptake) can be beneficial to phytoplankton, this strategy also leads to increased grazing pressure by microzooplankton (Lucas et al. 2007). Indeed, the low average biomass throughout the study region is mostly likely due to microzooplankton grazing pressure, although there are no data to confirm this.

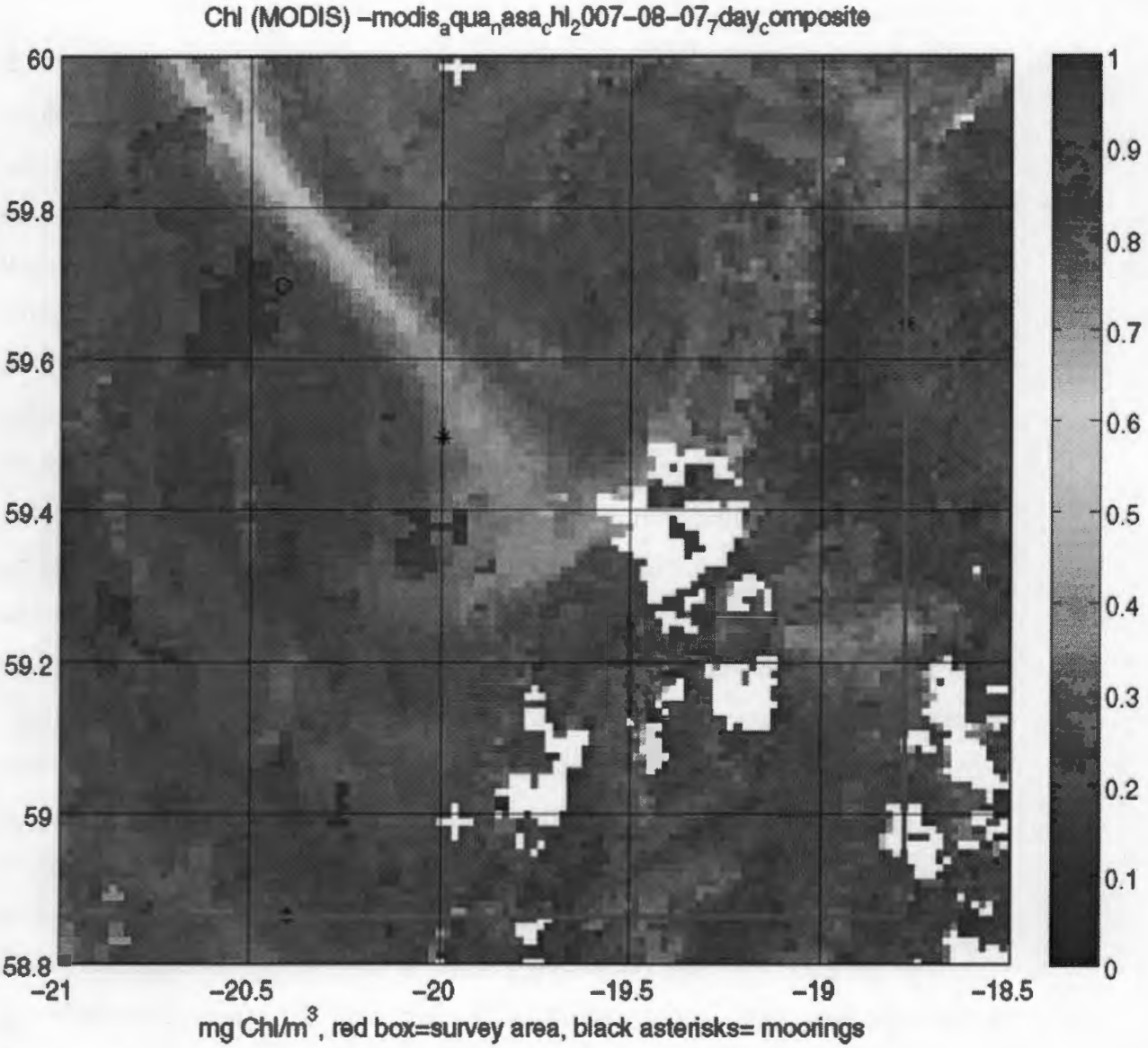

Figure 10: An ocean colour composite showing the productive jet and eddy Dipole

The satellite image above confirms the general and overall distribution of low chlorophyll-a concentrations, although the streak of higher chl-a water associated with the strong south-easterly flow between the eddy dipoles is clearly evident, suggesting that such flow is either advecting nutrients into the study region from the north west, or that the turbulent thermocline associated with strong currents is injecting nutrients into surface waters from below. However, without measurements of vertical turbulence, this remains a speculative comment.

5. Nitrogen uptake rates

The oceans – as has already been stated – play a major role in the global carbon cycle; they are the earth's largest active reservoir of carbon as well as the principle sink for anthropogenic CO_2 (Hays et al. 2005). This is for the most part due to the efficiency of the 'biological pump', which is primarily driven by processes which create particulate organic matter (POM). Primary production by phytoplankton dominates this process. The flux of organic material sinking to depth plays a vital role when considering the path of CO_2 (strength of the pump) in the ocean. However, export flux is notoriously difficult to measure directly and is generally estimated indirectly through quantifying the amount of primary production (phytoplankton growth) that is fuelled by the upward flux of nitrate (Yool et al. 2007). This is usually done by determining the fraction of primary production that will eventually constitute export. This fraction is made up of the proportion of nitrate (new production) relative to ammonium (regenerated production) as described by the 'f-ratio' (Yool et al. 2007). New production is based on nitrogen uptake which is 'new' to the euphotic zone (i.e. it originates from below the euphotic zone such as nitrate) whereas regenerated production is based on the uptake of regenerated/excreted nutrient production by decomposition and excretion (Yool et al. 2007). A region where uptake is predominantly based on new production will have high export production and a region dominated by regenerated production will have low export production.

The significance of this is that regions with high export are characterised by short, efficient food chains and 'patches' of ocean which act as CO_2 sinks to the atmosphere, while regions with low export production are dominated by long, inefficient food chains and may even act as a source of CO_2 to the atmosphere (Lucas et al. 2007). High export regions are typically dominated by larger celled organisms such as diatoms which function best in high nutrient regions with adequate light; however, in low export regions there will typically be a shift to smaller celled organisms (phytoflagellates and picoplankton) which due to a high surface to volume ratio are able to withstand low nutrient, low light conditions (Martin et al. 2001).

Factors which potentially could limit phytoplankton growth include factors such as light intensity and nutrient (specifically Nitrate and Phosphate) concentration (Beardall et al. 2001, Pennock and Sharp 1994). Light intensity is a dominant factor which limits phytoplankton growth; low irradiances within deep, mixed layers will limit growth even in high nutrient conditions. Nitrate uptake (new production) has a higher light dependency than ammonium or other forms of reduced nitrogen uptake (Cochlan et al., 1999 cited in Lucas et al. 2007), such that a reduced f-ratio can be expected with decreasing depth-related irradiance.

Nutrient concentration is an equally important factor to consider. Silicate limitation specifically affects community structure and thus ecosystem function. Reduced silicate concentrations (as has already been mentioned) leads to a dominance of smaller celled organisms but also increased phytoplankton mortality due to grazing (Lucas et al. 2008).

Iron is another (micro) nutrient which can severely limit phytoplankton growth and specifically phytoplankton nitrogen metabolism (Timmermans et al. 1994). Nitrate uptake and its subsequent reduction to NH_4^+ require the enzymes nitrate and nitrite reductase which are both iron-dependent processes because iron is needed as a co-factor for these enzymes (Timmermans et al. 1994). A region which is iron limited will again lead to a community dominated by small organisms able to access limited iron.

5.1 Nitrate and ammonium uptake

Ammonium uptake rates at all stations exceed nitrate uptake throughout the majority of the water column, demonstrating the overall significance of regenerated rather than new production - during summer months at least. However, at a few stations, nitrate uptake exceeds or equals ammonium uptake at a few depths, typically concurrent with higher chl-a concentrations that are diatom-dominated. The implication of this is that ammonium regeneration mediated by microzooplankton grazing is generally able to supply sufficient nitrogen to meet photosynthetic and stoichiometric needs, but where phytoplankton (diatom) growth rates exceed reduced N demand, nitrate becomes utilised (Lucas et al. 2008).

There are some phytoplankton species, as well as several kelp species, where the dark uptake of nitrate is significant (Anderson and Lucas 2007). The physiological explanation for this is that firstly, it is not light dependent in the same way that photosynthesis is, and that if an intracellular nitrate pool can be established during darkness, this becomes available to support and to stoichiometrically balance photosynthetic carbon fixation the following day (Anderson and Lucas 2007). However, in this study, dark nitrate uptake rates are consistently very low and remain relatively constant throughout the water column, forming just 1.31% of total N uptake. This value perhaps suggests that dark nitrate uptake could be considered negligible when considering the balance between ammonium and nitrate uptake (see f-ratio data).

Overall, most stations fall within a close range of each other with respect to integrated total N uptake rates (mmol m^{-2} h^{-1}). However, station 16285B exhibits uptake values that are appreciably higher than the rest this corresponds with a higher overall chl-a biomass (see figure 5j). Once again, integrated water column uptake rates are dominated (71.66%) by regenerated ammonium, reflecting the relative unimportance of nitrate uptake.

5.2 f-ratio and export production

Historically at least, the f-ratio ($\rho NO_3/\rho \Sigma N$) has been used to describe the amount of production available for export, either to zooplankton grazers, or for vertical export into the deep ocean. F-ratio values for this study, whether from profiles or from integrated uptake rates are almost all <0.5 (see table 1 and 2), confirming firstly that nitrogen nutrition is based primarily on reduced N, but indicating also that export production is generally <50% of overall production – at least in summer. However, the data generally shows higher f-ratios in the surface waters relative to depth because of the greater light dependency of nitrate uptake relative to ammonium uptake. Overall, therefore, the study region is characterised by low export production.

It is however important to note that the f-ratio may not be a totally accurate description of the amount of production available for export. At the best of times, quantifying the strength of the biological pump is complicated due to all the confounding factors such as the need for accurate sampling requires instruments that are able to operate at demanding depths, sampling sinking material for at least a month. For this reason export is largely estimated indirectly by determining the fraction of primary production that will eventually make up export. Phytoplankton use nutrients that are recycled from particulate organic matter (before it sinks) which puts scientists in danger of double-counting (Yool et al, 2007).

Evidence has recently been presented for euphotic layer nitrification rates, which suggests that due to nitrate produced through the oxidation of ammonium (nitrification) confusing the count of 'new' nitrate, using the f-ratio to estimate export rates is not as reliable as previously thought.

Until recently, it has been thought that the process of nitrification occurred entirely at depth. It is the depth separation which has allowed scientists to define 'new' and 'regenerated' primary production, where new production is

fuelled by nitrate which reaches the surface waters from depth while regenerated production comes from ammonium recycled within the euphotic zone (Yool et al. 2007). So 'regenerated' nitrate is converted to 'new' nitrate only beneath the 'permanent thermocline', if nitrification occurs in the surface waters, this nitrate is defined as 'regenerated nitrate'. Yool et al. (2007), discovered that nitrification can 'substantially distorts estimates of 'new' production.

However, the f-ratio is still a very useful concept in describing phytoplankton community structure (provided certain assumptions can be made; that a steady state is maintained, that no N storage occurs in surface waters and that there is minimal euphotic layer nitrification) and thus whether a particular 'patch' of ocean will act as a source or a sink of CO_2 to the atmosphere (Anderson & Lucas, 2008).

Conclusion

Chlorophyll-a biomass in the study region is generally low in the euphotic zone, reaching a subsurface maximum at about 25-50m depth. Production in the study region is dominated by regenerated production with overall f-ratios all falling below 0.5. However at the majority of the stations the euphotic zone is characterised by higher f-ratios (0.4-0.5), indicating - as would be expected due to nitrate uptake being more light dependent than ammonium uptake. It appears that phytoplankton in this region are silicate limited which would lead to a shift in community structure to smaller celled organisms not dependent on silicate for their structure (such as diatoms). This confirmed by low f-ratio values indicating that the water column is dominated by regenerated production normally associated with smaller celled organisms which migrated down through the water column when nutrients become depleted in the surface waters to take advantage of the small amounts of nutrients that diffuse over the nutricline from the deep, nutrient rich waters below.

Thus, it can be said that the study region in the Icelandic Basin could have undergone a community shift from larger celled organisms, with short efficient food chains and waters dominated by new production to one with smaller

celled organisms, long, inefficient food chains and waters dominated by regenerated production. This is significant due to the fact that the Icelandic Basin is considered one of the most productive regions in the world and supports the economically important Cod fishery.

Acknowledgments

I would like to thank Mike Lucas for input into this project; his advice has been invaluable.

References

(1) Anderson, T.R. & Lucas, M.I. 2007. Upwelling Ecosystems. National Oceanography centre, Southampton, United Kingdom.

(2) Beardall, J., Young, E. and Roberts, S. 2001. Approaches for determining phytoplankton nutrient limitation. *Aquatic Sciences*, **63**: 44-69.

(3) Chisholm, S.W., Falkowski, P.G. & Cullen J.J. 2001. Dis-Crediting Ocean Fertilization. *Science,* **294**: 309-310.

(4) Dugdale, R.C. Goering, J.J. 1967. Uptake of new and regenerated forms of nitrogen in primary production. *Limnology and Oceanography,* **12**: 196-206.

(5) Dugdale, RC., Wilkerson, FP., 1986. The use of ^{15}N to measure nitrogen uptake in eutrophic oceans; experimental considerations. *Limnology and Oceanography* **31**: 673-689.

(6) Dugdale, R.C., Wilkerson, F.P., Minas, H.J., 1995. The role of a silicate pump in driving new production. *Deep-Sea Research. I. Oceanographic Research Papers*, **42(5)**: 697–719.

(7) Falkowski, P.G., Barber, R.T. & Smetacek. V., 1998. Biogeochemical controls and feedbacks on ocean primary production. *Science*, **281**: 200-206.

(8) Falkowski, P., Scholes, R.J., Boyle, E., Canadell, J., Canþeld, D., Elser, J., Gruber, N., Hibbard, K., Högberg, P., Linder, S., Mackenzie, F. T., Moore III, B., Pedersen, T., Rosenthal, Y., Seitzinger, S., Smetacek, V. & Steffen W., 2000. The Global Carbon Cycle: A Test of Our Knowledge of Earth as a System. *Science*, **290**: 291-296.

(9) Francois, R., Honjo, S., Krishfield, R., Manganini, S. 2002., Factors controlling the flux of organic carbon in the bathypelagic zone of the ocean. *Global Biogeochemical Cycles*, **16(4)**: (art. 1087).

(10) Glibert, P.M., Biggs, D.C. and McCarthy, J.J., 1982a. Utilization of ammonium and nitrate during austral summer in the Scotia Sea. *Deep-Sea Research I.* **29**: 837-850.

(11) Glibert, P.M., Lipshultz, F., McCarthy, J.J., Altabet, M.M., 1982b. Isotope dilution models of uptake and remineralisation of ammonium by marine phytoplankton. *Limnology and Oceanography* **27**: 639-650.

(12) Hays, G. C., Richardson, A. J. and Robinson, C. 2005. Climate change and marine plankton. *Trends in Ecology and Evolution*, **20(6)**: 337-344.

(13) Holmes, R.M., Aminot, A., Kerouel, R., Hooker, B.A., Peterson, B.J., 1999. A simple and precise method for measuring ammonium in marine and freshwater ecosystems. *Canadian Journal of Fisheries and Aquatic Sciences* **56 (10):** 1801-1808.

(14) Martin, A. P., Richards, K. J. and Fasham, M. J. R. 2001. Phytoplankton production and community structure in an unstable frontal region. *Journal of Marine Systems*, **28**: 65-89.

(15) Mitchell-Innes B.A., Silulwane, N. & Lucas, M.I., 2001. Variability of Chlorophyll Profiles on the West Coast of Southern Africa in June/July 1999. *Southern African Journal Science,* **97**: 246-250

(16) Moore C.M., Mills, M.M., Milne, A., Langlois, R.., Achterberg, E.P., Lochte, K., Geider, R.J., & La Roche, J., 2006. Iron limits primary productivity during spring bloom development in the central North Atlantic. *Global Change Biology*, **12:** 626-634.

(17) Painter, S.C., Sanders, R., Waldron, H.N., Lucas, M.I., Malcolm, E. Woodward, S., & Chamberlain, K., 2008. Nitrate uptake along repeat meridional transects of the Atlantic Ocean. *Journal of Marine Systems*, In Press, Corrected Proof

(18) Painting, S.J., Moloney, C.L. & Lucas, M.I., 1993. Simulation and Field-Measurements of Phytoplankton-Bacteria- Zooplankton Interactions in the Southern Benguela Upwelling Region. *Marine Ecology-Progress Series*, **100(1-2):** 55-69.

(19) Pennock, J. R. and Sharp, J. H. 1994. Temporal alternation between light- and nutrient-limitation of phytoplankton production in a coastal plain estuary. *Marine Ecology Progress Series*, **111**: 275-288.

(20) Probyn, 1987. Ammonium regeneration by microplankton in an upwelling environment. *Marine Biology* **37**: 53-64.

(21) Probyn, T.A., 1992. The inorganic nitrogen nutrition of phyto-plankton in the southern Benguela: new production, phyto-plankton size and implications for pelagic food webs. In: Benguela trophic functioning. *South African Journal of Marine Science,* **12**: 411-420.

(22) Richardson, A.J., Verheye, H.M., Herbert, V., Rogers, C. & Arendse, L.M. 2001., Egg production, somatic growth and productivity of

copepods in the Benguela current and Angola-Benguela Front. *South African Journal of Science*, **97**: 251-256.

(23) Sanders, R., Morris, P., Stinchcombe, M., Seeyave, S., Venables, H. J., Lucas, M. I. & Moore, C. M. 2007. New production and the f-ratio around the Crozet Plateau in austral summer 2004-5 diagnosed from seasonal changes in inorganic nutrient levels. *Deep-Sea Research II*, **54**

(24) Smetacek, V., 1998. Diatoms and the Silicate factor. *Nature*, **391**: 224-225.

(25) Tilstone, G.H., Smyth, T.J., Rees, A.P., Blondeau-Patissier, D., Holeton, C., Moore, C.M., Lucas, M.I., Groom, S.B., Joint, I., 2007. Measured and satellite estimates of new and primary production in the northern North Atlantic from 1998 to 2005. *Deep Sea Research I* (in press)

(26) Timmermans, K. R., Stolte, W. and de Baar, H. J. W. 1994. Iron-mediated effects on nitrate reductase in marine plankton. *Marine Biology*, **121**: 389-396.

(27) Welschmeyer, N.A., 1994. Fluorometric analysis of chlorophyll-a in the presence of Chlorophyll-B and Phaeopigments. Limnology *and Oceanography*, **39(8)**: 1985-1992.

(28) Yool, A., Martin, A. P., Fernandez, C. & Clark, D. R. 2007. The significance of nitrification for oceanic new production. *Nature*, **447**: 999-1002